COMPARISONS OF TOTAL MAGNETIC INTENSITY GRIDS, COMBINED USING GRIDMERGE, WITH TWO INDEPENDENT DATASETS

Peter R. Milligan, Brian R.S. Minty, Tony Luyendyk & Andrew Lewis

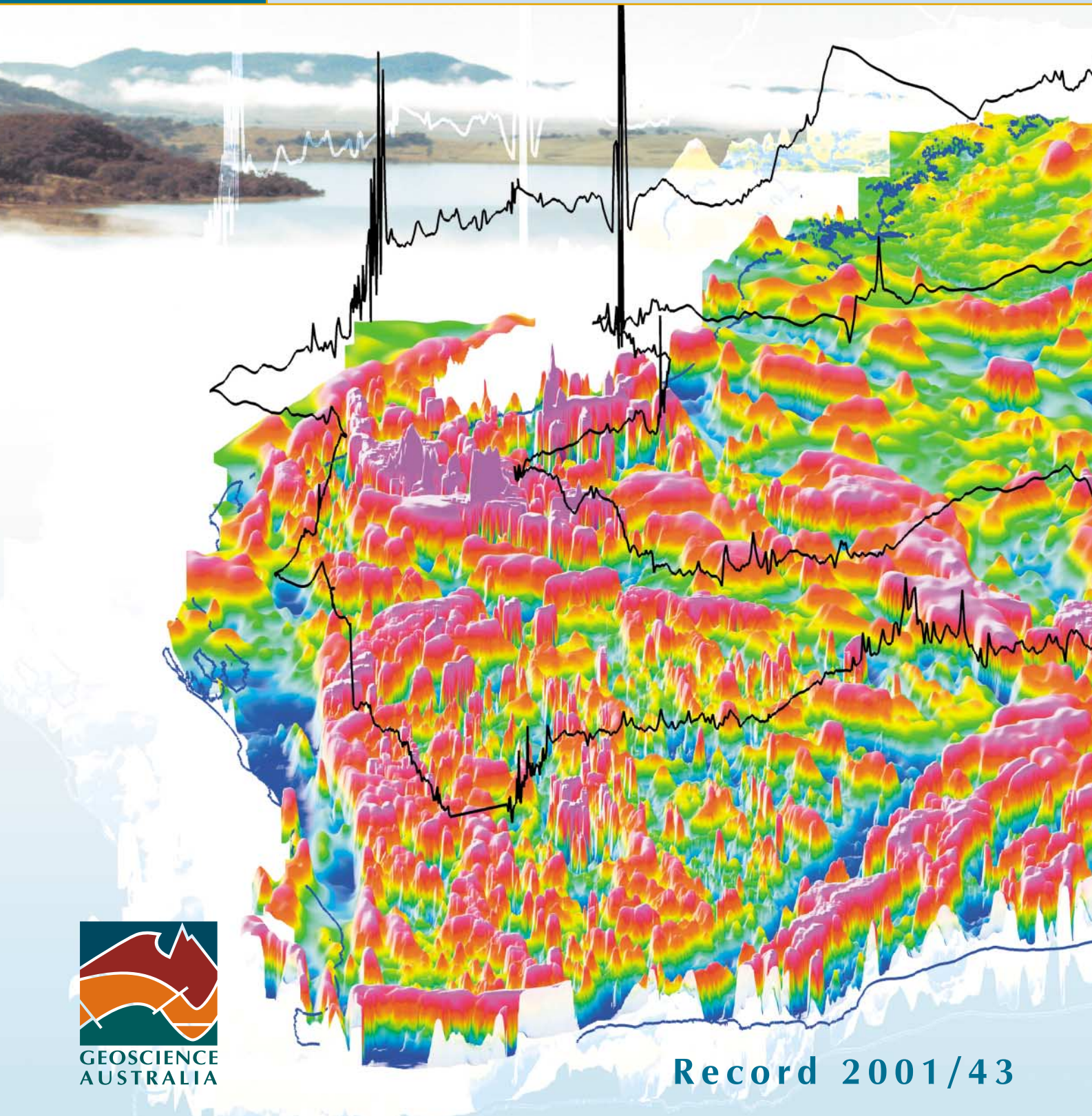

GEOSCIENCE AUSTRALIA

Record 2001/43

SPATIAL INFORMATION FOR THE NATION

CONTENTS

Cover Picture

Three-dimensional view of the total magnetic intensity (TMI) of Western Australia. Profiles of the AWAGS flight data are shown above the image.

ABSTRACT

Regional and continental compilations of magnetic survey data are commonly undertaken, as national survey databases grow. There is now a complete coverage of the Australian continent with magnetic survey data, and the grid data for the individual surveys have been merged into a single grid. Digital processing, enhancement and display of such composite grids enable features of all scales to be reliably mapped, and greatly facilitate the interpretation of tectonic features and geological provinces.

Grid data for the individual projects are usually matched by minimising in a least-squares sense the discrepancies between grid values along common rows and columns, using low order polynomials. High frequency residual differences are later smoothed out using a Laplacian operator. Joining such grids sequentially leads to long-wavelength errors in the final result, as the polynomials are propagated throughout the merged grid.

Early in 1990 two control traverses were flown around the Australian mainland to help in the correction of the spurious long wavelengths. Also deployed across the whole continent at this time was a large array of over 50 three-component fluxgate magnetometers, which formed the Australia Wide Array of Geomagnetic Stations (AWAGS) experiment. These instruments recorded the time-varying components of the geomagnetic field (the “diurnals”), which could then be removed from the airborne control traverses (the AWAGS traverses). Data for these traverses have been reprocessed, and now form a definitive dataset which can be used to test the quality of merged magnetic data.

A second magnetic dataset is available to provide an independent comparison with airborne magnetic grids covering large areas of Australia. During the period 1967 to 1975 total magnetic field measurements were made at approximately 8000 stations across Australia as part of the Third-order Regional Magnetic Survey. Although these are only spot measurements, with no close diurnal control, there are sufficient of them over large areas to provide a statistically useful comparison with the airborne gridded data. An attempt has been made to diurnally correct the Third-order data by using observatory data. However, the Third-order data cannot be used to provide reliable information for wavelengths less than a few thousand kilometres. In some cases they help to identify individual survey grids that are anomalously tilted.

During 2000/2001 a new automatic method of merging gridded airborne magnetic data was developed by Geoscience Australia. This involves considering all the grids at once, and treating the requirement that they match together in the best possible way as a single inverse problem. Both ‘DC’ and low-order polynomials can be applied to grids during the process. The program *Gridmerge* undertakes these tasks, as an independent entity within the Intrepid geophysical processing system.

Regional compilations of airborne magnetic data (from the Yilgarn area of Western Australia, the Tanami-Arunta area of the Northern Territory, the Curnamona region of South Australia and New South Wales and all of Western Australia) are used to compare the results of *Gridmerge* with the test datasets. For the Western Australia merged data, the standard deviation from the AWAGS traverse data is ±66.15 nT, measured over more than 5000 km. This deviation is greatly reduced by using the AWAGS traverses as a control on the merging process, and standard datasets such as these should always be used, if available, in forming composite magnetic grids.

The quality of the individual grids has a major impact on the quality of the final merged result. In particular, removal of the incorrect IGRF from survey data results in poor merges, and the spurious tilts can be propagated into other grids. *Gridmerge* produces high quality results very efficiently for the combination of aeromagnetic data, when compared with older methods.

1. INTRODUCTION

Airborne magnetic surveys were first undertaken in Australia in 1951, and since then the whole continent has been covered to varying degrees of precision. Summaries of the Australian database are contained in Tucker *et al.* (1988) and Hone *et al.* (1997). Similar surveys have been undertaken across the other major continental landmasses of the world, with the subsequent publication of continent wide datasets and maps. There are several advantages to having a single coherent compilation: the data are more amenable for digital enhancement and display; large features are more reliably mapped; and the interpretation of major tectonic features and geological provinces is facilitated. In general, such synopses provide a valuable contribution to research into continent-scale processes of the lithosphere (e.g. Hinze *et al.*, 1988; Reford *et al*., 1990; Barritt, 1993; Black *et al*., 1995).

The first edition of the Magnetic Map of Australia was published in 1976 (BMR, 1976) by BMR (the Bureau of Mineral Resources, Geology and Geophysics, now Geoscience Australia). Although incomplete, and published in contour map form, this was the forerunner of the new series of datasets and maps which are published under the title of the 'Magnetic Anomaly Map of Australia'. The new series is being released in both digital and hardcopy form (as enhanced pixel-image maps): the first edition was published in 1993 (Tarlowski *et al*., 1992, 1993), the second edition in 1995 (Tarlowski *et al.*, 1995) and the third edition in 1999 (Milligan and Tarlowski, 1999).

Data from individual surveys, which are combined to form the composite datasets, were acquired over the years on a project basis, with each project mainly consisting of the acquisition of data over one or more 1:250 000 map sheet areas. The grid data for the individual projects were combined by minimising in a least-squares sense the discrepancies between grid values along common rows and columns, using low order polynomials. High frequency residual differences were later smoothed out using a Laplacian operator (Tarlowski *et al.,* 1992).

While each of these editions represented a step forward in the addition of higher quality data and extra coverage, the methods used to merge the individual grid data were essentially the same. From a starting grid, other grids were successively joined by operations on the boundary overlaps, where these overlaps consisted of just one grid row or column of overlap (the grids were preprocessed to provide a perfect one point row/column overlap). The low-order polynomials selected to fit the boundary differences were applied to the entire grid being matched in a direction perpendicular to the overlap boundary. This process propagated long wavelength errors across the whole compilation (if grids were joined in a circle by this process, the start and end grids would be poorly matched).

The flaw in the merging process as described above was recognised, and to help in the correction of the spurious long wavelengths two control traverses were designed and flown around the Australian mainland early in 1990 (Tarlowski *et al.*, 1996). Timing for the acquisition of these traverses was designed to coincide with the deployment of a large array of over 50 three-component fluxgate magnetometers across the whole of mainland Australia. This was the AWAGS experiment (Australia Wide Array of Geomagnetic Stations), a collaborative research project between The Flinders University of South Australia and Geoscience Australia (Chamalaun and Barton, 1990; Chamalaun and Walker, 1982). This coincidence of ground stations and the airborne acquisition was critical so that the time-varying components of the geomagnetic field (the "diurnals") could be monitored and removed from the airborne data.

Tarlowski *et al.* (1996) discussed in detail the diurnal correction of the AWAGS control traverses and their subsequent comparison with the grid data of the Magnetic Anomaly Map of Australia, second edition (1995), and the dewarping of the grid data. They used the differences between the control traverses and the magnetic

grid to produce a difference grid, interpolated and extrapolated across the whole continent, to correct the long wavelength components in the original grid. This process is not a good solution, because there is little control supplied by the AWAGS traverses perpendicular to the flight direction. The interpolation/extrapolation between and outside the traverses is applied over hundreds of kilometres. As a consequence, the resulting dataset and images still contain spurious intermediate (100s km) and long (1000s km) wavelength information. An important use of the AWAGS control traverses is that they can be compared with a grid generated in a new grid merging technique, which is described in Chapter 4.

A second magnetic dataset is available to provide an independent comparison with airborne magnetic grids covering large areas of Australia. During the period 1967 to 1975 vector magnetic field measurements were made at approximately 8000 stations across Australia in the Third-order Regional Magnetic Survey (van der Linden, 1971; Dooley and McGregor, 1982; Dooley, 1985). Although these are only spot measurements, with no close diurnal control, there are sufficient of them over large areas to provide a statistically useful comparison with the airborne gridded data.

During 1999 a new automatic method of merging gridded airborne gamma-ray spectrometric data was developed by Geoscience Australia (Minty, 2000). This involved considering all the grids at once, and treating the requirement that they all match together in the best possible way as a single inverse problem. Radiometric data require the adjustment of two parameters, a scaling and a base-level shift. Magnetic data do not require scaling, as the measurements are universally made in magnetic field units (nT) with either calibrated or absolute total-field instruments. However, they require base-level, or 'DC', shifts. Also, magnetic grids can have spurious tilts in the data, due to such causes as inadequate levelling, poor removal of the International Geomagnetic Reference Field (IGRF), or inaccurate removal of diurnal variations. The method developed for radiometrics has now been extended to allow the automatic merging of magnetic grid data into composite datasets. Both DC and low-order polynomials can be applied to grids during the process (Minty *et al*., in prep.). The program *Gridmerge* undertakes these tasks, as an independent entity within the Intrepid geophysical processing system (http://www.dfa.com.au/).

This report compares both the AWAGS control traverse data and the Third-order data with composite magnetic grids merged using the new process. The largest composite grid available at present is that of the Magnetic Map of Western Australia (Mackey *et al*., 2000). The data for this map were merged using a trial version of *Gridmerge*. It was subsequently discovered that there were large warps in those merged data also. After much development and testing of the *Gridmerge* software, many improvements in the algorithms have been made, to the stage where it is now providing reliable, stable results within the limitations of the method.

This report summarises several aspects of development of the AWAGS and Third-order datasets, and provides results of:

- generating a diurnally corrected set of AWAGS traverses (Chapter 2),
- generating a diurnally corrected Third-order dataset (Chapter 3),
- comparing two diurnally corrected datasets against each other (Chapter 3),
- comparing the results of *Gridmerge*, using the diurnally corrected datasets (Chapters 4 and 5),
- testing *Gridmerge* using the datasets as controls (Chapters 5 and 6),
- testing that the Third-order data have sufficient precision to fill in between the AWAGS lines,
- testing that the datasets can be used to remove erroneous tilts from individual project grids,
- testing *Gridmerge* in a theoretical sense—analysing how well the method works with perfect data.

The authors of this report have contributed vitally to the *Gridmerge* program: Brian Minty (Geoscience Australia Minerals Division) developed the method; Tony Luyendyk (Geoscience Australia Minerals Division) implemented the method into the robust *Gridmerge* program; and Andrew Lewis (Geoscience Australia Urban Geoscience Division, Geomagnetism) made the diurnal corrections to the Third-order data.

2. AWAGS CONTROL TRAVERSES

Introduction

The AWAGS control traverses were flown under contract for BMR in two circuits around Australia during January 27–February 26, 1990. Survey specifications were carefully designed to avoid, where possible, areas of high magnetic gradient in the crustal magnetic field. The acquisition height above ground level was 150 m, which at the time was the height at which most of the regional magnetic data across Australia were acquired. Figure 2.1 shows the flight-line traverses.

The aircraft was equipped with a Caesium magnetometer, which sampled the total magnetic field at 0.5 s intervals. At an average aircraft speed of 290 km/h, this translates to a ground sampling interval of about 40 m. Navigation was by the satellite Global Positioning System (GPS), accurate to about 50 m. The accuracy and precision of the magnetometer is 0.01 nT.

These data were originally processed and diurnally corrected by Tarlowski *et al.*, (1996), for the de-warping of the second edition of the Magnetic Anomaly Map of Australia. For this study, the airborne traverse data have been reprocessed using a method similar to that of Tarlowski *et al*. (1996).

Preliminary Processing

For the data to be useful for comparison with airborne magnetic grid datasets, some preliminary processing is required. This involves making sure the data are spike free, any data gaps are flagged, the appropriate International Geomagnetic Reference Field (IGRF) has been removed, and a diurnal correction has been applied.

The processed data supplied by the contractor had an elevation of zero altitude used for the calculation of the IGRF values. For the purposes of this report, the raw data have been used, and the IGRF value removed for each data sample using the height above sea-level to calculate the reference field. The diurnal correction is more complicated to calculate, as there are effectively more than 50 base-station magnetometers to take into account, over 31 days of flying. This correction is described in more detail in the next section.

Diurnal Correction

The data from the AWAGS base-stations have been further processed to provide a ‘definitive’ set of X, Y, Z component values (the original base-station processing is described in Tarlowski *et al.*, 1996). This later processing is detailed in Welsh and Barton (1996), and it is this dataset that has been used here to provide diurnal control for the flight-line data. Welsh and Barton used the following processing procedure to produce the X, Y, Z component values:

1. compensate for clock errors,
2. remove spikes,
3. remove step shifts
4. smooth abnormally noisy segments,
5. correct for instrument drift,
6. adjust each station to a common (DGRF) reference level.

The final dataset comprised of 58 stations — 54 were from portable 3-component fluxgate magnetometers (Chamalaun and Walker, 1982) and four were AGSO’s permanent observatories. The locations of the instru-

ments are shown on Figure 2.1.

For each of the portable magnetometers, data were recorded with a one minute sampling interval, and a least count sensitivity of 1 nT. The permanent observatories provided accurate one-minute absolute data. Full details concerning the instruments, and the deployment and processing of the data, can be found in Chamalaun and Walker (1982) and Welsh and Barton (1996). The three-components of magnetic data recorded by each instrument are combined into total-field variations, and it is this total-field value which is further processed here to produce the diurnal correction.

The errors in the final diurnal correction are difficult to estimate. The AWAGS magnetometers sample to a least count resolution of 1 nT, but their long-period precision is poor. Considerable 'cleaning' of the data has been undertaken, as already noted. It is estimated that the long-term precision is no better than ±3 nT for any particular sample. Sample to sample precision will be of the order of ±1 nT.

As stated previously, the diurnal correction using multiple base-station instruments is more complicated than correction using just one instrument. In the single instrument case, the base-station total-field data can be subtracted from the survey flight data. As absolute values of the field are not required in the final survey data after IGRF and diurnal correction, this procedure is adequate.

However, with more than one base station, estimating the correction at flight locations requires interpolation between base stations, and a base-level is required for each instrument. This latter criterion is very important. Imagine, for example, that one base-station was located at a position with a crustal anomaly of 100 nT, and another was located near a crustal anomaly of 1100 nT, 100 km away. If an interpolation was performed at the mid-way point of 50 km, using the absolute recordings of the instruments, the diurnal to be subtracted would be of the order of 600 nT plus/minus the interpolated difference in the diurnal variation component, which would typically be a few 10s of nT at most. Thus, huge errors would be introduced into the diurnal

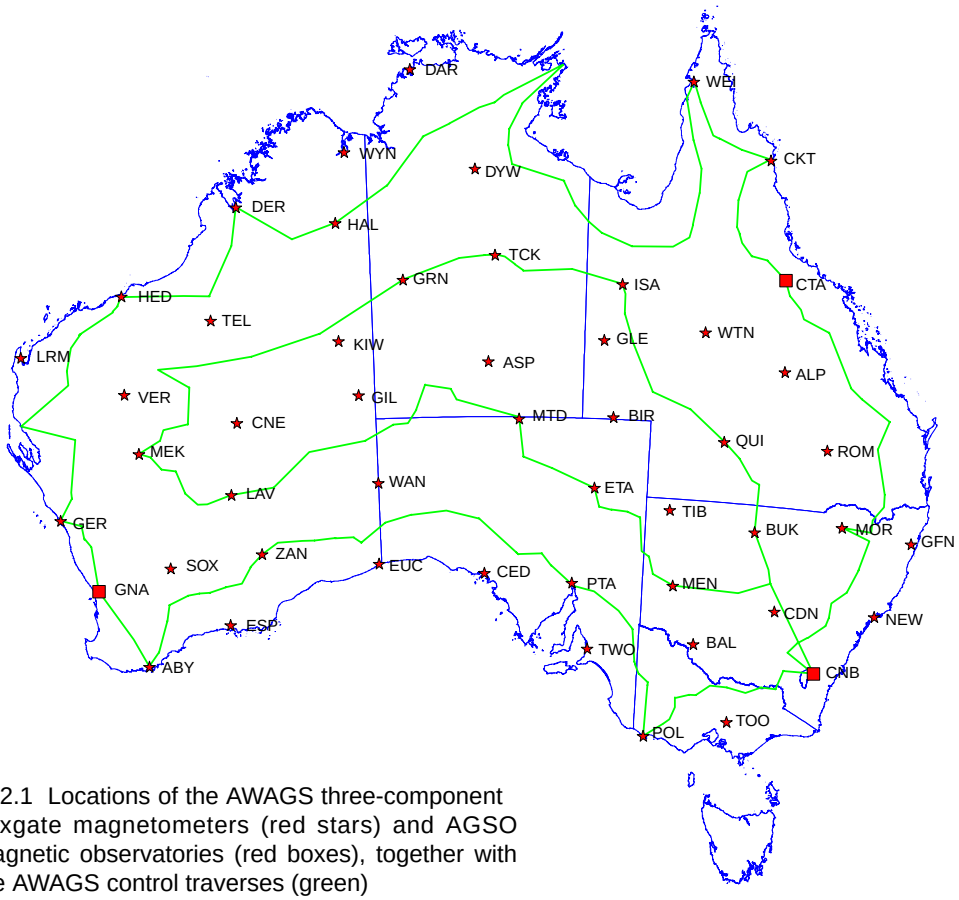

Figure 2.1 Locations of the AWAGS three-component fluxgate magnetometers (red stars) and AGSO magnetic observatories (red boxes), together with the AWAGS control traverses (green)

correction through the differences in crustal magnetisation at the base-station locations. For a single base station case, this does not matter, as it merely results in a DC offset to the whole survey.

In order to overcome this problem, a base-level for each base-station must be defined that represents, as far as possible, the undisturbed (or quiet) value of the geomagnetic field in terms of short-period temporal variations. For the daily variation, which arises from currents in the ionosphere on the sunlit hemisphere of the Earth, the values of the field for a few hours after midnight local time are considered undisturbed. These can then be averaged, and the resultant value used as a base. However, the midnight values will vary significantly depending upon the longer term state of the field. For example, for several days after a magnetic storm, the whole field of the Earth will be at a significantly different level from a quiet period.

The approach taken here is to use the average of the midnight values of the first few quiet days in the undisturbed period of the field just before the commencement of flying the AWAGS traverses. Any significant deviation of midnight values from this average value then represents a real departure of the field from a base value, and will be taken into account in the calculation of the diurnal. This approach may not be as rigorous as that used in the original reduction by Tarlowski *et al.*, (1996), but the differences are small.

Once the base value for each total-field instrument record has been estimated, the diurnal variation is interpolated in both space and time along the flight paths of the control traverses. This is achieved by forming a set of grids at 1° intervals interpolated from the total-field values of the base-stations across Australia for every minute of the total duration period of the AWAGS flights. This set of grids is stored in one three-dimensional array. A computer program has been written to perform the interpolation process, providing the desired result of a diurnal value for every sample of the control flights.

Examples of the diurnal correction will be shown in a later section, where the flights are used in the comparison process with merged airborne grids. Figure 2.2 below shows some examples of the daily variation at eight AWAGS sites across Australia. As can be observed, daily variation ranges of the order of 60–80 nT are not uncommon, particularly at coastal observatories, where the amplitudes are enhanced by induction in the conducting sea-water (the ‘Coast Effect’, e.g. Parkinson, 1959, 1962; Whellams, 1996; Hitchman, 1999; Hitchman *et al*., 2000).

A major assumption made in the diurnal correction process is that the variations are smoothly varying between the magnetometer sites, and can be interpolated in a smooth fashion. This assumption is valid for the longer period changes of the daily variation and its harmonics, but is almost certainly not true for shorter period events related to magnetic storm activity (Milligan *et al*., 1993; Milligan, 1995). A major reason for this is the presence of conductive structures in the Earth, including the sea. These structures have spatial wavelengths less than the average spatial separation distance of the AWAGS magnetometers, and are thus not well sampled. Ideally, magnetic surveys are flown during periods of quiet magnetic activity. In the case of the AWAGS flights, there was little choice as to their timing, and unfortunately the magnetic field during February 1990 was more disturbed than during the months before and after (Tarlowski *et al.*, 1996).

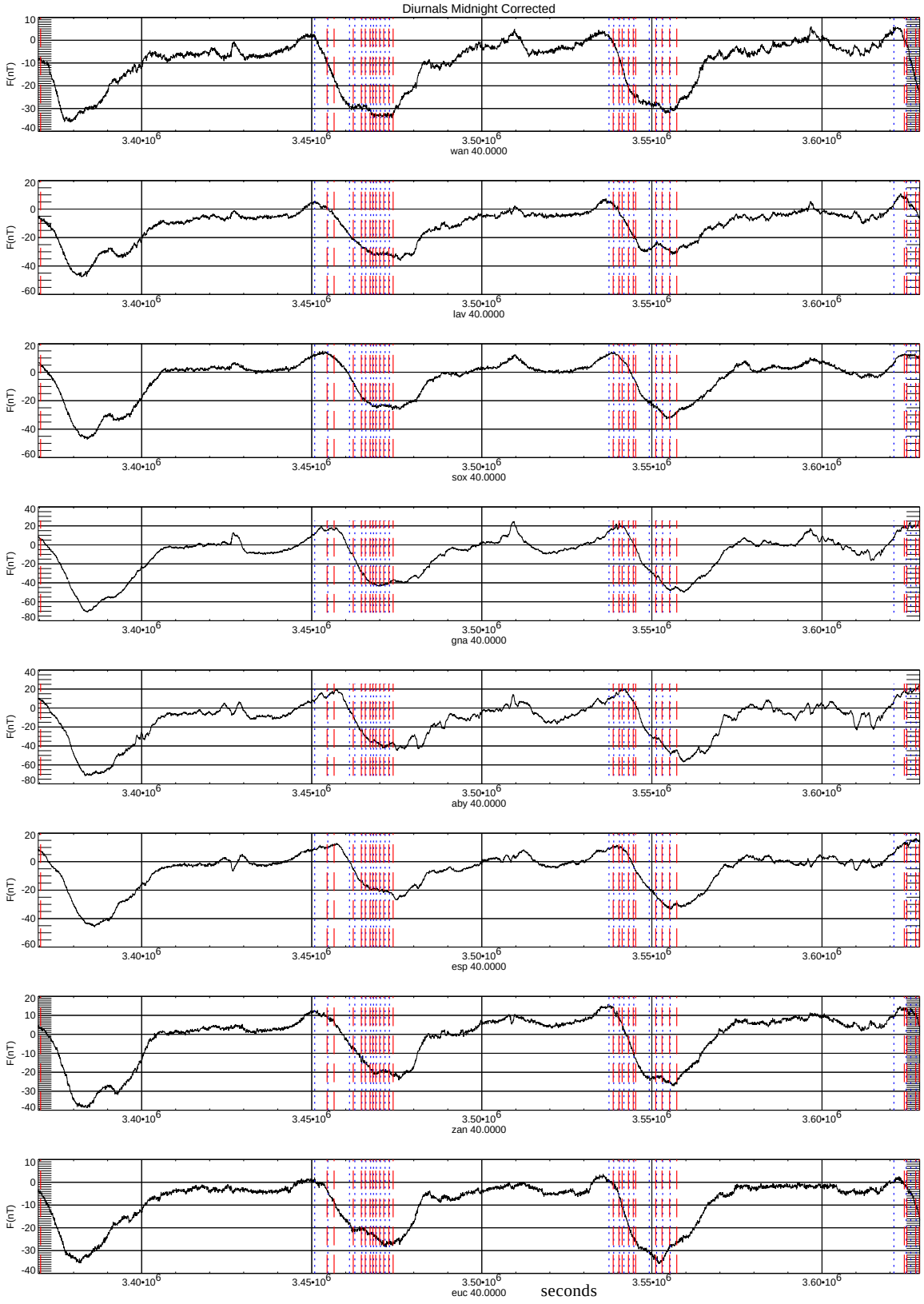

Figure 2.2. An example record (over three days) for selected AWAGS magnetometer sites. The start (blue line) and end (red line) locations of AWAGS control flights are also shown. It is an unfortunate aspect of airborne surveying that it has to be done during the middle of the day, when the maximum daily variation is also experienced. This is clearly shown in these plots.

3. THIRD-ORDER DATA

Introduction

Measurements of the vector magnetic field, which comprise the Third-order dataset, were made at approximately 8000 spot sites across Australia (including Tasmania and some nearby offshore islands) between 1967 and 1975 (van der Linden, 1971; Dooley and McGregor, 1982; Dooley, 1985). Using a nominal station spacing of 15 km, this survey was undertaken by the Observatories Branch of BMR, with the primary purpose of improving the quality of magnetic charts. Although absolute instruments were used to make the observations, there was no diurnal control. The term 'third order' refers to the lowest level of accuracy in a hierarchy of geomagnetic (and geodetic) surveying, which begins with 'first order', now called 'repeat station' surveying. The definition of a Third-order station is as follows (from van der Linden, 1971):

> A third-order station is one at which the field, or one of its components, has been observed once with an accuracy of about 20 gammas (or the equivalent angle) and which is located only by a map.

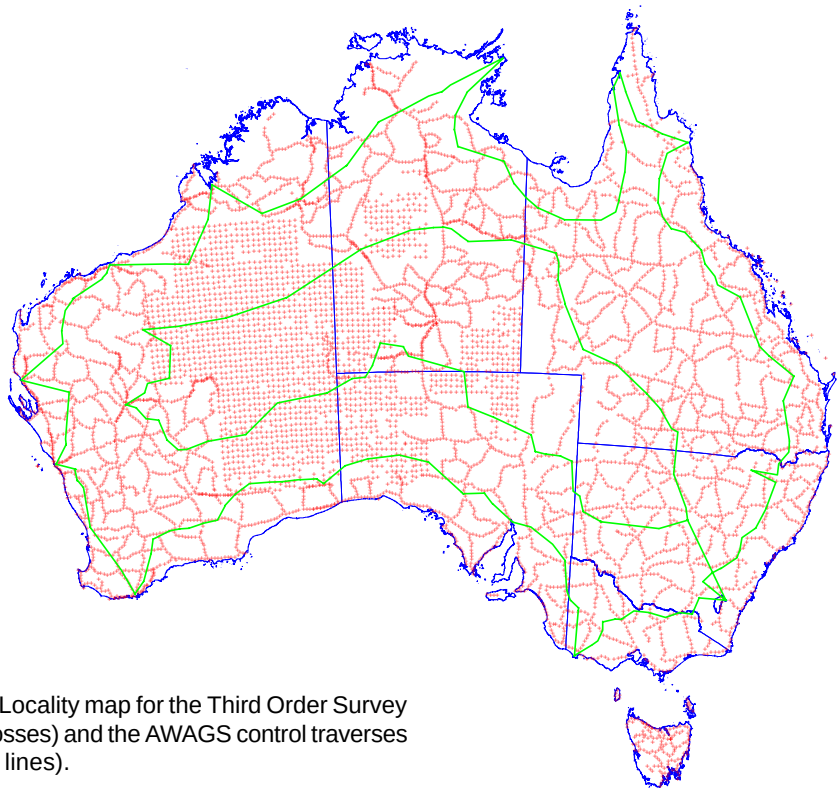

Figure 3.1. Locality map for the Third Order Survey (red crosses) and the AWAGS control traverses (green lines).

Three components of the field were measured: declination (D), the horizontal field magnitude (H) and the total-field (F). D was measured using a compass theodolite (Wild T0 instruments), H by a Quartz Horizontal Magnetometer (QHM) and F by a proton precession magnetometer (Elsec-595 instruments). Other components could then be computed using standard formulae.Only F is of interest here for the comparison with airborne surveys.

Over most of the country a single two-person field crew executed the survey with one vehicle. Magnetic stations were sited along roads, and the locations and altitudes of each station were read from topographic

maps and aerial photographs. In isolated areas of central Australia two survey crews operated with helicopter transportation, and stations were set out on a square grid based on map sheets. Timing of the observations was by radio time signals, at least for the 1968 and 1969 legs in eastern Australia. Two measurements were made at each site, and if they agreed the survey party moved on to the next station.

Van der Linden (1971) makes some interesting observations about the measurements, which are relevant for consideration of the overall accuracy of the Third-order data:

> In some areas local magnetic disturbances gave problems in the drawing of isomagnetic lines. The distance between stations of 16 kilometres or more is generally too large to determine whether anomalies are related. Therefore only large-scale anomalies were indicated. In most cases the lines were drawn by taking running means of three or four stations, and eliminating stations with obvious local disturbance.

As this paragraph suggests, for such a survey, where large parts of it are made along convenient roads, there are major sampling problems. The crustal magnetic field contains much power at very short wavelengths (hundreds to thousands of metres), which, at the sampling interval of tens of kilometres, becomes aliased into longer wavelengths. This will be discussed in more detail in a later section.

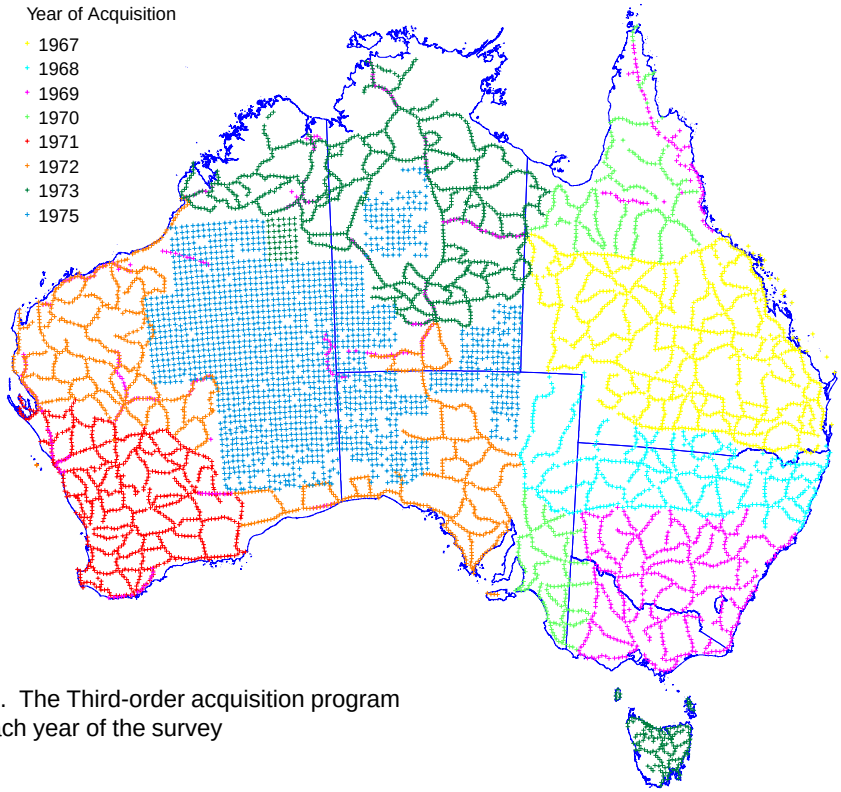

Figure 3.2. The Third-order acquisition program for each year of the survey

Figure 3.1 shows the Third-order station locations for the complete set of observations made between 1967 and 1975, with the AWAGS control flight lines also shown, in green. Figure 3.2 shows the localities for each year observations were made.

Uses of the Data

For the last 30 years the main use of the Third-order dataset has been for developing geomagnetic field models in the Australian region. The dataset is used as one of the primary sources of information in the Australian Geomagnetic Reference Field (AGRF) model, and has also been used in simpler models and hand-drawn charts since 1970 (Finlayson, 1973). The data may be useful for identifying long wavelength crustal anomalies, as discussed later.

For most applications of the Third-order data, what is required is a measure of the undisturbed or 'normal' field value at each station. Given the numerous sources that contribute to the magnetic field measured at the Earth's surface, it is always difficult to determine the normal field level at any location with complete confidence. Often the best available approximation to the normal field that can be directly measured is the field value around local midnight on a magnetically quiet night that is unaffected by any storm recovery events. Unfortunately, these measurements are difficult to make (see also Chapter 2).

Problems with the Survey

Observations were made during daylight hours. This was an operational necessity since direct observation of the sun was used for determining declination. Consequently, the observational data are subject to quiet day variations. The survey was also conducted irrespective of the level of solar and magnetic activity, and no attempt was made to monitor local magnetic variations (1968 was an annual averaged sunspot maximum, 1976 was a minimum (http://www.ips.gov.au/background/richard/ssn-vals.html).

Observations made during magnetically active periods could, in extreme cases, be hundreds of nT different from the normal field level. The magnetic conditions during the Third-order survey are illustrated in crude form in Figure 3.3. The plot shows the planetary K index at the time of each Third-order station occupation as a coloured dot. A K value of 3 or greater indicates disturbed magnetic conditions; a K value of greater than 7 indicates a severe magnetic storm.

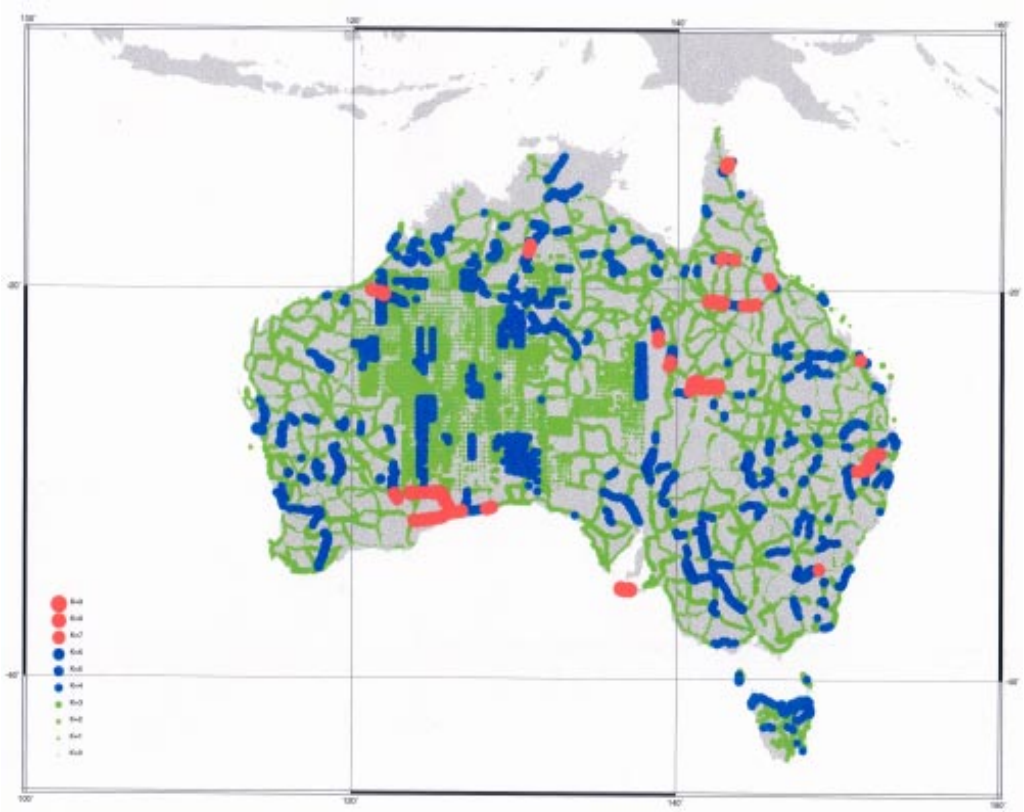

Figure 3.3. Magnetic activity at the time of recording of the Third-order data

In general, stations were located along roads. This sampling strategy has biased the data; for example, roads usually avoid large hills, and large hills are often made of exposed magnetic basement. Also, no magnetic gradients were measured in the vicinity of the stations.

There is little documentation on the survey operations, which leads to uncertainties about the quality of the data. For example, QHMs often have instrument corrections of the order of 50 nT. These corrections need to be applied to the observed data to yield absolute values of the magnetic field. From the information that can be gleaned, it appears the preliminary corrections were applied to the data, but no specific details or figures

can be retrieved. The original survey data forms were found, but the majority of these do not include instrument identifications, so even if the final instrument corrections were available it would be difficult to apply them with confidence.

Correcting the Data

As discussed above, if all the stations in the Third-order survey could be corrected to normal field levels then the survey data would be more useful as input into regional field models and to study long-wavelength crustal anomalies. To apply such a correction two major sources of "contamination" must be removed — the quiet day variation and any magnetic storm disturbance effects.

The quiet day (Sq) variation is typically a regular sinusoidal-like cycle throughout the daylight hours with a typical magnitude of the order of 50 nT in the intensity components and 10 minutes of arc in the angular components. The magnitude of the Sq variation depends on local time and the magnetic activity of the day. Storm disturbance effects can be many hundreds of nT during large storms and are generally independent of local time (i.e. they are Universal Time (UT) events).

For accurate corrections to be applied to the survey data, a detailed knowledge of the Sq variation at each station and an accurate record of the magnetic storm disturbance variations at the station are required. In short, a magnetic variometer record of at least several days is required at each station. Obviously this is not available. The next best alternative is to derive information from the magnetic records at the nearest geomagnetic observatory. During the time of the Third-order survey (1967–1975) there were three magnetic observatories in the Australian region: Toolangi, Gnangara and Port Moresby. All these observatories had analogue photographic variometers, and their records have been hand digitised and stored on computer files as mean hourly values.

When correcting for magnetic storm disturbances, the magnetic observatory record may provide reliable information, since storm effects usually occur at the same UT time at different locations. The matter of amplitude and phase are another question, because disturbances do not generally have the same amplitudes and phases at different locations, due in part to local crustal variations in electrical conductivity. Even if storm disturbances were the only disturbing fields, a corrected field value could not be achieved to better than a few tens of nT of the normal field value.

In addition, Sq is a local-time variation and has a different character at different locations; the greatest changes of its major morphology are latitude dependent (Hitchman, 1999; Hitchman *et al*., 1998). Given these uncertainties, any form of correction to the data could probably only get to within a few tens of nT of the normal field values at best, so it is not worth developing an elaborate correction scheme when a simple one may well produce results that are almost as good.

Methods

The observatory data mean hourly values (MHVs) from Toolangi (TOO), Gnangara (GNA) and Port Moresby (PMG) have been plotted and inspected. In general, the observatory data are of fair quality, although there are some large sections of missing data, several obvious base-level shifts, and the TOO data, in particular, contain many spikes — probably an artefact resulting from poor digitising techniques. Obvious base-level shifts and spikes were edited from the data.

The normal field values for each month of the period 1967–1975 for each of the three observatories have been adopted by selecting field values from around local midnight on International Quiet Days (IQDs) that appear to be unaffected by any preceding storm disturbances. These picks of the components H, D and F were made by experienced practitioners.

Not all months have suitable quiet day data; these months have been omitted. The adopted data have been plotted and inspected for outliers, which have been subsequently removed.

Using these three data sets the normal field value at each observatory for any time in the interval 1967 to 1975 can be calculated by linear interpolation of the nearest neighbouring monthly values. Also, the difference between the actual measured value of the field at the observatory and the normal field can then be calculated for any specified time. Because we have only mean hourly values, linear interpolation can be used for times that lie between hourly means.

The observatory data are now used to predict the value of the normal field at each Third-order station. This is done by calculating the difference between the normal and actual fields at the three observatories for the measurement times of each of the Third-order stations. If these differences are spatially and temporally systematic then interpolated differences are used to correct the actual field at each of the Third-order stations.

The simplest model that can be fitted to the difference data from the three available observatories is a planar surface. In order to determine if a planar surface would produce acceptable results recent observatory data were tested.

Testing the Method

Using the observatory network as it existed in 1991 in Australia (1992 was the last year of PMG), a planar surface was fitted to the instantaneous difference at GNA, Canberra (CNB) and PMG. (TOO ceased operation in 1979). The predicted value of the difference was then evaluated at the location of the Learmonth (LRM) and Charter Towers (CTA) observatories. Of course the instantaneous 'actual' field at LRM and CTA was also known (these are the equivalent of the Third-order data), hence a value of the normal field can be derived.

At LRM and CTA the normal field could also be adopted from the observatory records. Hence the predicted normal field value derived through the correction process could be compared to the adopted normal field value to evaluate the suitability of the correction method.

Three different times were selected from 1991 to test the method in different magnetic conditions.

- 05:00 UT on 07 March 1991 had a K index of 2
- 09:00 UT on 21 March 1991 had a K index of 3
- 03:00 UT on 25 March 1991 had a K index of 7

The results of the tests are presented in the tables below. All tabulated values are in nT or decimal degrees. In each case, the *derived normal field* values in the table should be compared to the highlighted *adopted normal field* values for LRM and CTA. The *derived normal field = actual field + correction*.

05:00 7 March 1991 K = 2 (quiet).

Actual field value (MHV)

Observatory	*H*	*D*	*F*
CNB	23639	12.625	58629
GNA	23167	-3.002	58524
PMG	35937	6.638	43046
LRM	29513	-0.4183	53300
CTA	31737	7.855	49698

Adopted normal field (from MHV plots March 1991)

Observatory	*H*	*D*	*F*
CNB	23656	12.52	58630
GNA	23198	-3.045	58582
PMG	35914	6.602	43031
LRM	**29529**	**-0.445**	**53350**
CTA	**31737**	**7.790**	**49701**

Derived normal field

Observatory	*H*	*D*	*F*
LRM	29530	-0.4	53354
CTA	31731	7.8	49692

Magnitudes of the corrections to determine the *derived* normal field

Observatory	*H*	*D*	*F*
LRM	16.7	-0.0	53.9
CTA	-5.8	-0.1	-5.6

Table 3.1. Comparison of the results show that the adopted normal field values and the derived normal field values are within 10 nT and 0.04 degrees. The test period had quiet magnetic conditions (K index 2).

09:00 21 March 1991 K = 3

Actual field value (MHV)				Adopted normal field (from MHV plots March 1991)			
Observatory	*H*	*D*	*F*	*Observatory*	*H*	*D*	*F*
CNB	23693	12.565	58635	CNB	23656	12.52	58630
GNA	23233	-2.982	58570	GNA	23198	-3.045	58582
PMG	35959	6.623	43065	PMG	35914	6.602	43031
LRM	29570	-0.413	53350	**LRM**	**29528**	**-0.445**	**53350**
CTA	31779	7.823	49723	**CTA**	**31737**	**7.79**	**49701**

Derived normal field				Magnitudes of the corrections to determine the *derived* normal field			
Observatory	*H*	*D*	*F*	*Observatory*	*H*	*D*	*F*
LRM	29532	-0.5	53352	LRM	-38.0	-0.1	2.0
CTA	31737	7.8	49702	CTA	-41.8	-0.0	-21.4

Table 3.2. Comparison of the results show that the adopted normal field values and the normal field values derived through the correction process are within 5 nT and 0.06 degrees.

03:00 25 March 1991 K = 7 (very disturbed).

Actual field value (MHV)				Adopted normal field (from MHV plots March 1991)			
Observatory	*H*	*D*	*F*	*Observatory*	*H*	*D*	*F*
CNB	23382	12.657	58568	CNB	23656	12.52	58630
GNA	22863	-3.067	58433	GNA	23198	-3.045	58582
PMG	35696	6.67	42840	PMG	35914	6.602	43031
LRM	29232	-0.448	53137	**LRM**	**29529**	**-0.445**	**53350**
CTA	31488	7.91	49535	**CTA**	**31737**	**7.79**	**49701**

Derived normal field				Magnitudes of the corrections to determine the *derived* normal field			
Observatory	*H*	*D*	*F*	*Observatory*	*H*	*D*	*F*
LRM	29548	-0.4	53336	LRM	316.3	0.1	198.8
CTA	31733	7.8	49676	CTA	244.5	-0.1	141.2

Table 3.3. Comparison of the results show that the adopted normal field values and the normal field values derived through the correction process are within 20 nT and 0.05 degrees.

These results indicate that for mean hourly value data this simple method of correction can produce field values that are within a few tens of nT of an adopted normal field value even during severely disturbed conditions.

Data Entry and Pre-Processing

In order to apply the correction to the Third-order dataset, there needs to be an observation time associated with every observation. The Third-order data file and the data in the Oracle database 'Third' (Chopra, 1989) only had a date, and not an observation time. However, observation times were recorded on the original field forms, and these have now been added to the digital database. During this process, other aspects of the data were checked (location, dates, etc.) and numerous problems and inconsistencies in the original data were identified and resolved before all possible geomagnetic elements were finally calculated.

Observatory Data

As mentioned above, some corrections had to be made to the mean hourly values observatory data from TOO, GNA and PMG. Most time consuming was the removal of spikes common in the TOO data. This was done by manually identifying the spikes on MHV plots and setting the offending data to a null value in the MHV files.

Applying the Corrections

The observatory mean hourly value data were linearly interpolated to calculate an instantaneous field value for the observatories at the time of the Third-order observation. Ideally, this interpolation is done across a one hour interval; however, due to the numerous spikes in the TOO data the interpolation was also allowed over a 2 hour interval in the case where one of the MHV data points was missing.

The corrections were applied to each magnetic component separately and all seven components were corrected where possible. Any Third-order station where at least one H, D or F component could not be corrected (perhaps due to missing observatory data) was recorded in a separate file. The locations of these

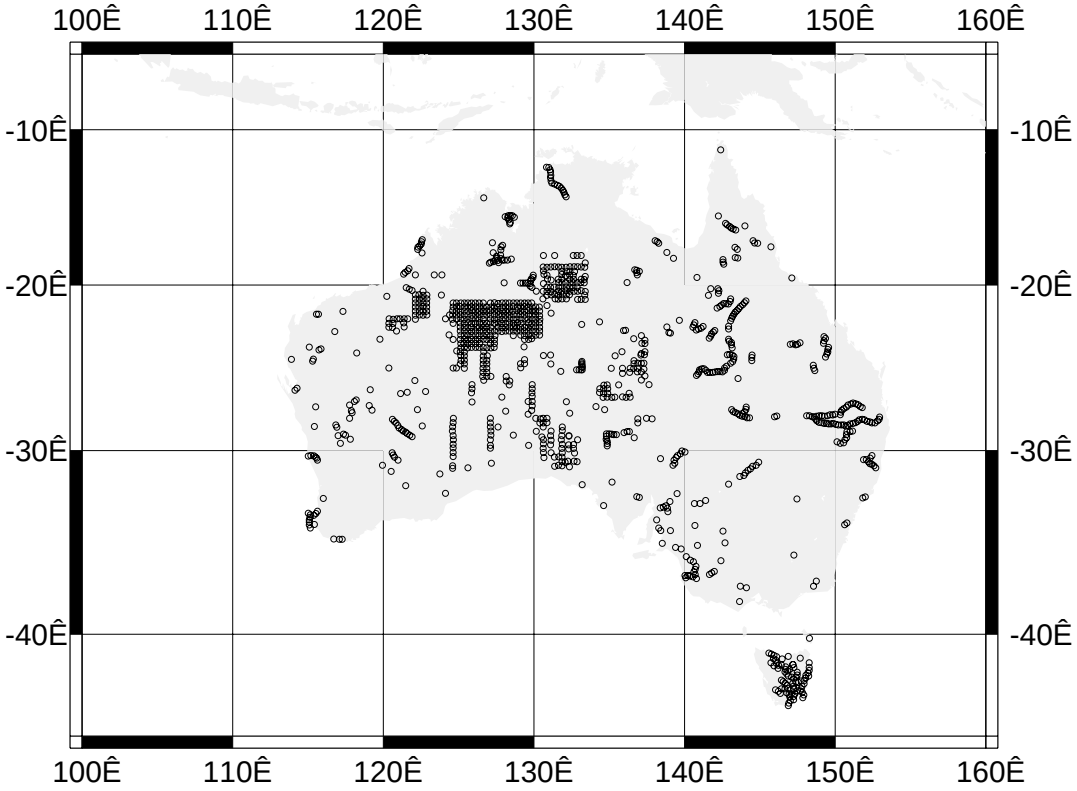

Figure 3.4. Plot of Third-order stations with at least one element uncorrected.

stations are plotted in Figure 3.4. The magnitude of each of the corrections was also recorded and inspected to identify any unusually large correction that might indicate problems with the input data. Histograms of the magnitude of corrections are presented in Figure 3.5.

IGRF Removal

Although the Third-order total-field measurements were made with a proton precession magnetometer, which provides absolute values of the field to 1.0 nT accuracy, the nature of the survey, including the wide time span for measurements, means that the data required further processing to allow detailed comparisons of the magnetic field at individual data sites with other datasets, such as those derived from airborne surveys. The reductions that had to be applied included the removal of an appropriate reference field model.

IGRF models have undergone an evolution over the decades, and although final DGRF (Definitive Geomagnetic Reference Field) models have been generated, the models for different epochs vary in accuracy. Therefore, the subtraction of an IGRF value for, say, 1967, from a measurement may not provide the same residual as the same measurement made at the same site in 1990 with the appropriate IGRF 1990 subtracted. This is

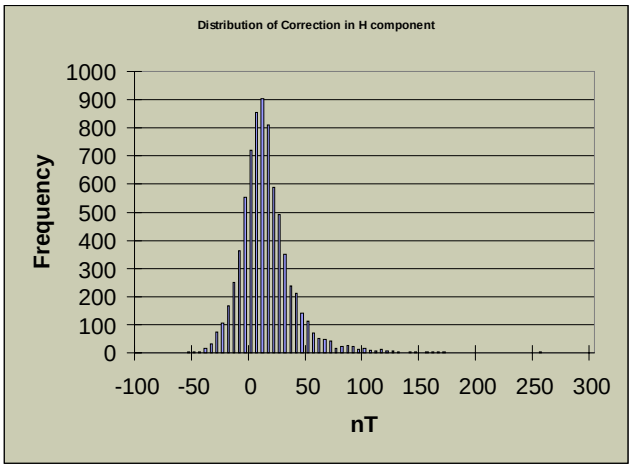

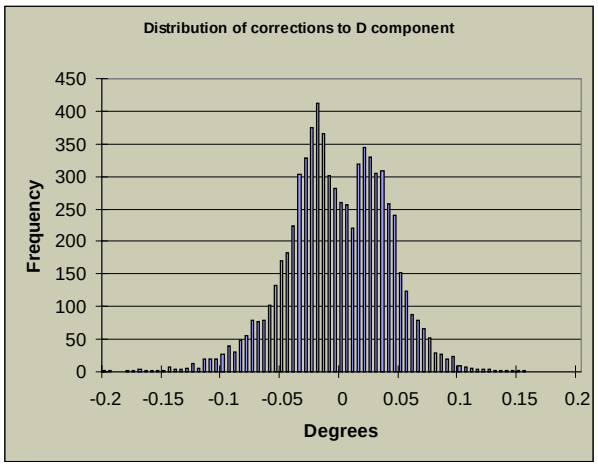

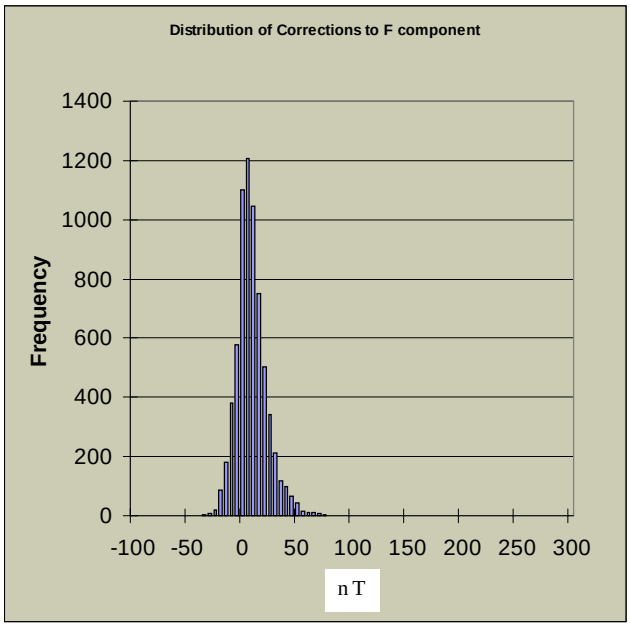

Figure 3.5. Histograms of the magnitudes of diurnal corrections applied to three components

assuming all other variabilities, such as the diurnal variation, are the same. It must be remembered that the IGRF is a best fitting global model to degree and order 10 of the Earth's field, and the southern hemisphere is lacking in measurement sites compared with the northern hemisphere.

AGSO and USyd (University of Sydney) are producing a new secular variation model for the Australian region, based on observatory values and repeat station survey data. This will be available shortly, and will provide much more reliable estimates of the secular variation for the update of survey data collected at differing epochs. Until the new model is available, the Third-order data used here have had the appropriate DGRF/IGRF removed for the date/time of acquisition.

Errors in the Third-order Data

From the foregoing discussion, it is clear that considerable errors remain in the processed Third-order data, which ideally should provide measurements of only the crustal magnetic field. There are errors due to variations in the removal of the IGRF, in the removal of diurnal variations, and also in the location of the measurement sites (which is important for detailed AWAGS profile comparisons). These were plotted from maps, and the accuracy must be to several hundred metres, at best. As previously mentioned, the horizontal gradients in the Earth's magnetic field over a few hundred metres can be tens to hundreds of nT, or thousands of nT in very active regions. This is a severe limiting factor on the accuracy of the final measurements, that can at best only be accurate to a few tens of nT, in areas of low gradients of the magnetic field. Note that the AWAGS control traverses are located to 10 m accuracy.

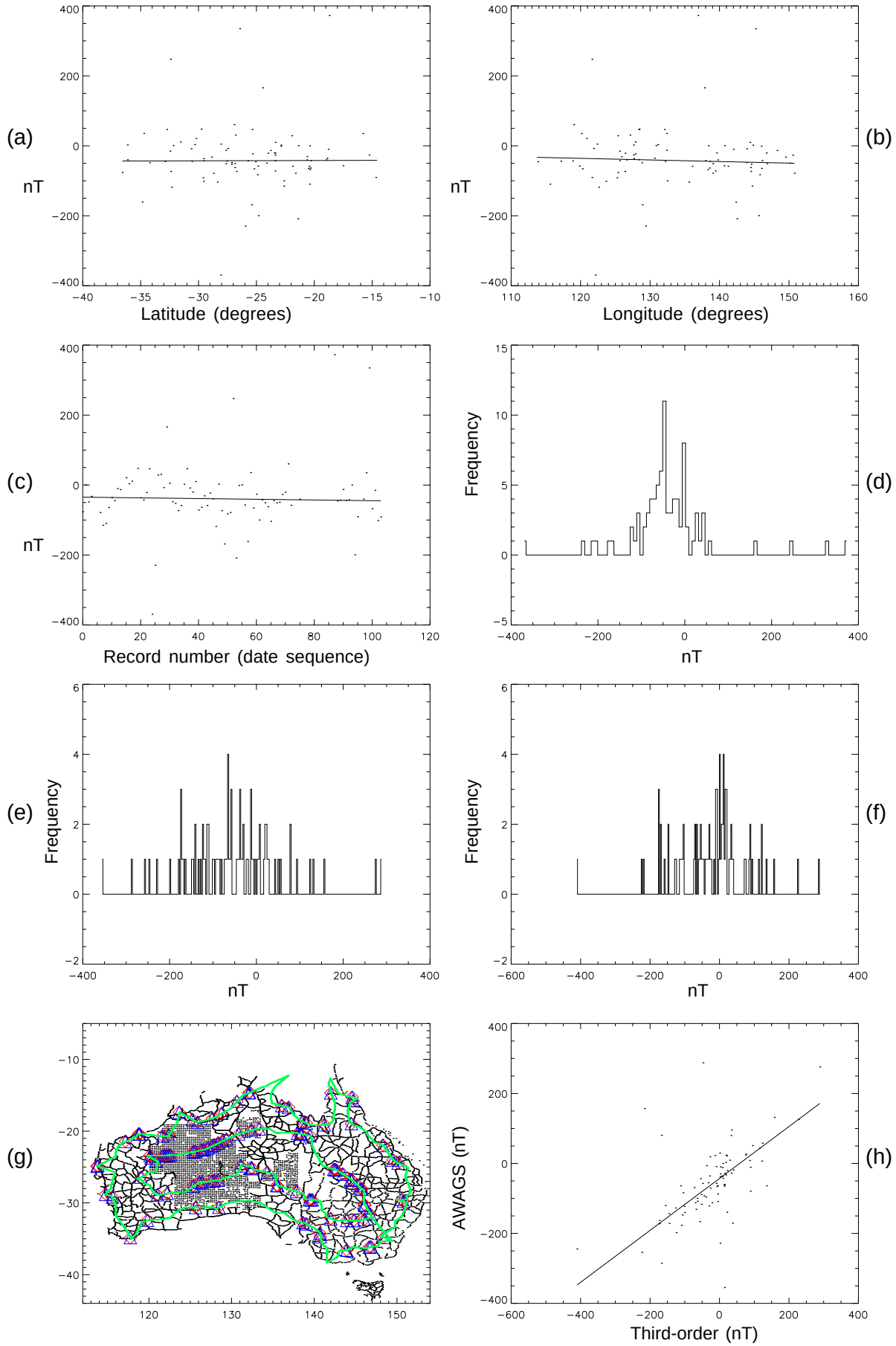

Figure 3.6. Comparison plots between diurnally corrected Third-order data and the AWAGS control flight data, for measurement sites that are closer than 0.003 degrees of arc and for which the horizontal gradient of the AWAGS data does not exceed 1.0 nT/80m. See text for details.

Comparison between the Third-order data and the AWAGS control line data

One way to test the accuracy of the residual Third-order measurements is to compare them with the AWAGS control flight values. In this process, the AWAGS sample nearest to each of the Third-order samples is found, and then a subset of the Third-order data is generated, based on the distance between these nearest samples. As no Third-order site is coincident with any AWAGS sampling point, this distance is chosen so that there are a reasonable number of points left to compare.

In the example that follows, the AWAGS flight data have been lightly smoothed with a three-point running average operator, and then the horizontal gradient calculated. The standard deviation of the gradient is 18 nT/80 m (the horizontal gradient is calculated on a fiducial basis, over two fiducial intervals). Some of the large extremes in the gradient will be accounted for by the calculation running over the ends of flight breaks. This is not taken into account, but data are rejected if the horizontal gradient exceeds 1.0 nT/80 m. The gradient is also only calculated along the direction of the flight line, and thus takes no account of gradients in any other direction.

Data are also rejected from the comparison if the distance between the Third-order site and the nearest AWAGS sample point exceeds 0.003 degrees of arc. This is approximately 300 m, depending upon the latitude, and provides approximately 86 data points for the comparison. Comparisons have been made using both the uncorrected and the diurnally corrected Third-order data. The results are explained in more detail below, and plots of the corrected results are shown in Figure 3.6.

There are several ways the data can be analysed to show how the two datasets relate to each other. Figure 3.6(a) is a plot of the residual differences and latitude, and Figure 3.6(b) the differences and longitude. Although there is significant scatter, there is only a small trend, as emphasised by the best-fitting line. These trends translate to about 2.5 nT in a north–south direction, and 23 nT in an east–west direction across the whole continent. Considering the history of the survey, and the corrections made, these results are good, and provide confidence in the further use of the data.

Figure 3.6(c) is a plot of the differences and record numbers, which are really equivalent to dates, as the data are stored in sequence. As the Third-order data were acquired over several years, with different instruments and observing personnel, this plot would show up any major shifts in the differences with regard to time. The small slope of the regression line suggests temporal effects are negligible.

Figure 3.6(d) is a histogram of the differences, centred close to zero as expected, as the IGRF values have been removed from both datasets and any other DC shift should be small. The diurnal corrections to F are relatively small (<50 nT, see Figure 3.5), and they are also small compared to the scatter in Figure 3.6(d). Histograms of the separate datasets are provided in Figures 3.6(e),(f). The Third-order data have a broader histogram than the AWAGS data, as might be expected given that they contain greater measurement errors. The correlation between the Third-order data and the AWAGS data is plotted in Figure 3.6(h).

The locations of the sites that have been used in this comparison are shown in Figure 3.6(g). Very similar results are obtained whether the raw data or corrected data are tested, showing that diurnally correcting the Third-order data has not significantly improved the data quality. There are some minor improvements, with slightly narrower histograms, but the differences are marginal.

Another test has been devised to check the validity of the Third-order data with the AWAGS control lines. The Third-order data have been averaged into “bins”. In this binning process, a compromise has been achieved between including as much short wavelength information as possible, and leaving enough data values to be averaged. Also, the smaller the bins, the more the aliasing involved.

In the example shown in Figure 3.7 the data have been binned into 2° bins and a thin plate spline surface generated. This surface is represented by the colour image shown in Figure 3.7; it passes through all the binned data values and can be compared with the AWAGS control flights. The comparison is shown in Figure 3.8. While there is some agreement between the two profiles, there are also significant sections where the

correlation is not good. This is probably due to the poor sampling of the Third-order data.

There is no significant degree 1 difference between the two profiles. That is, the continental scale gradients of the Third-order data and the control traverse are in agreement, as they should be if consistent IGRF values have been removed from both datasets.

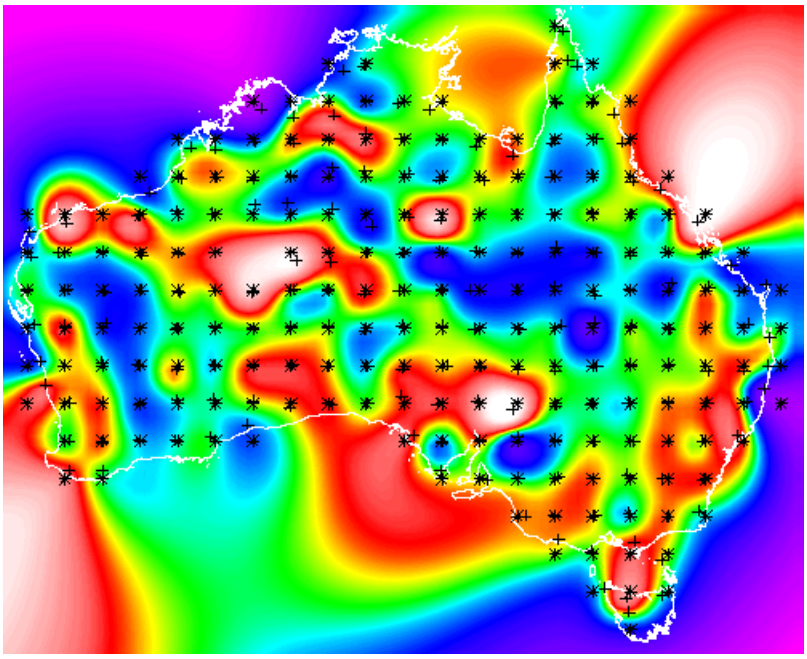

Figure 3.7. The thin plate spline surface generated from the binned Third-order data. The asterisks show centres of bins, and the crosses show data average centres.

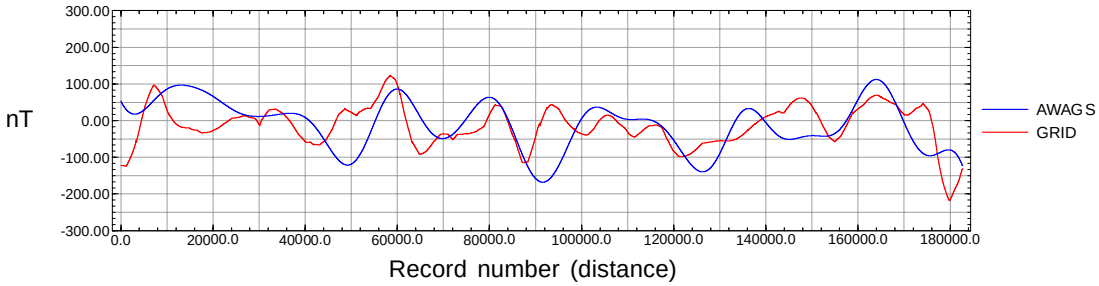

Figure 3.8. Comparison of the Third-order binned grid with the AWAGS outer flight line over Western Australia. Both profiles have been filtered to remove wavelengths less than 600 km. The width of the plot is approximately 4,500 km.

4. AWAGS COMPARISONS

Introduction

The best dataset available for comparison with merged grids is the AWAGS control traverse data. As discussed in Chapter 2, these data were acquired in a short time frame, with diurnal control, across the whole continent. They are accurate to within a few nT for all wavelengths, and thus also contain information for spherical harmonics greater than degree and order 10, which is where the IGRF values are truncated. Although this means that information is still contained in the data from the internal core field, as well as information mainly from the static crustal field, all airborne magnetic grid data have had the equivalent IGRFs removed, and so the comparison is valid.

Several sets of grids merged with the *Gridmerge* program are compared to the AWAGS control traverses. These grids range in size from a few merged 1:250 000 map sheet areas to the whole of Western Australia.

Method

Grid data for each of the surveys to be joined have been processed according to AGSO recommended specifications, with microlevelling, where appropriate, to remove linear short-wavelength artefacts associated with sampling along flight-lines. The grids have also been trimmed to remove ragged boundaries left after the gridding process.

The *Gridmerge* program is based on the grid merging method described by Minty (2000) for merging radiometric grids, and Minty *et al.* (in prep.) for merging magnetic grids. The method attempts to minimise the introduction of long-wavelength errors into large regional compilations by taking a holistic approach to the joining of survey grids. Rather than join grids sequentially, the levelling of all of the grids in the regional compilation is treated as a single inverse problem. The method uses the differences between survey grid values where grids overlap to estimate the necessary grid adjustments. For magnetic data, the method proceeds in three stages.

(a) A level shift is calculated for each grid so that the differences between grids in the overlap areas are minimised. These level shifts are then applied to the grids. This step is crucial to minimising long wavelength errors. Since all grid overlaps are used to estimate these level shifts, the inconsistencies between grids are effectively spread between all the overlap regions.

(b) Each grid is iteratively adjusted by removing a low-order polynomial surface to further minimise the differences in the overlap areas. This step adjusts grids that are tilted due to incorrect IGRF/DGRF adjustment or poor levelling.

(c) Any residual differences between grids in the overlap areas are ‘feathered’ prior to merging the grids. The feathering procedure uses a series of filter convolutions with successively smaller cut-off wavelengths to propagate residual errors in the overlap areas into the respective grids.

The method used for the comparison process is similar to that described for the comparison of the AWAGS control flight data with the Third-order dataset (Chapter 3). The grid under consideration is interpolated at each AWAGS traverse position for comparison and plotting.

Several results can be plotted along the sections of traverse that overlap the grid data. These include the AWAGS flight data, the diurnal variations, the data interpolated off the magnetic grid at the AWAGS traverse positions, and the difference between the AWAGS traverse data and the interpolated grid data. The profile

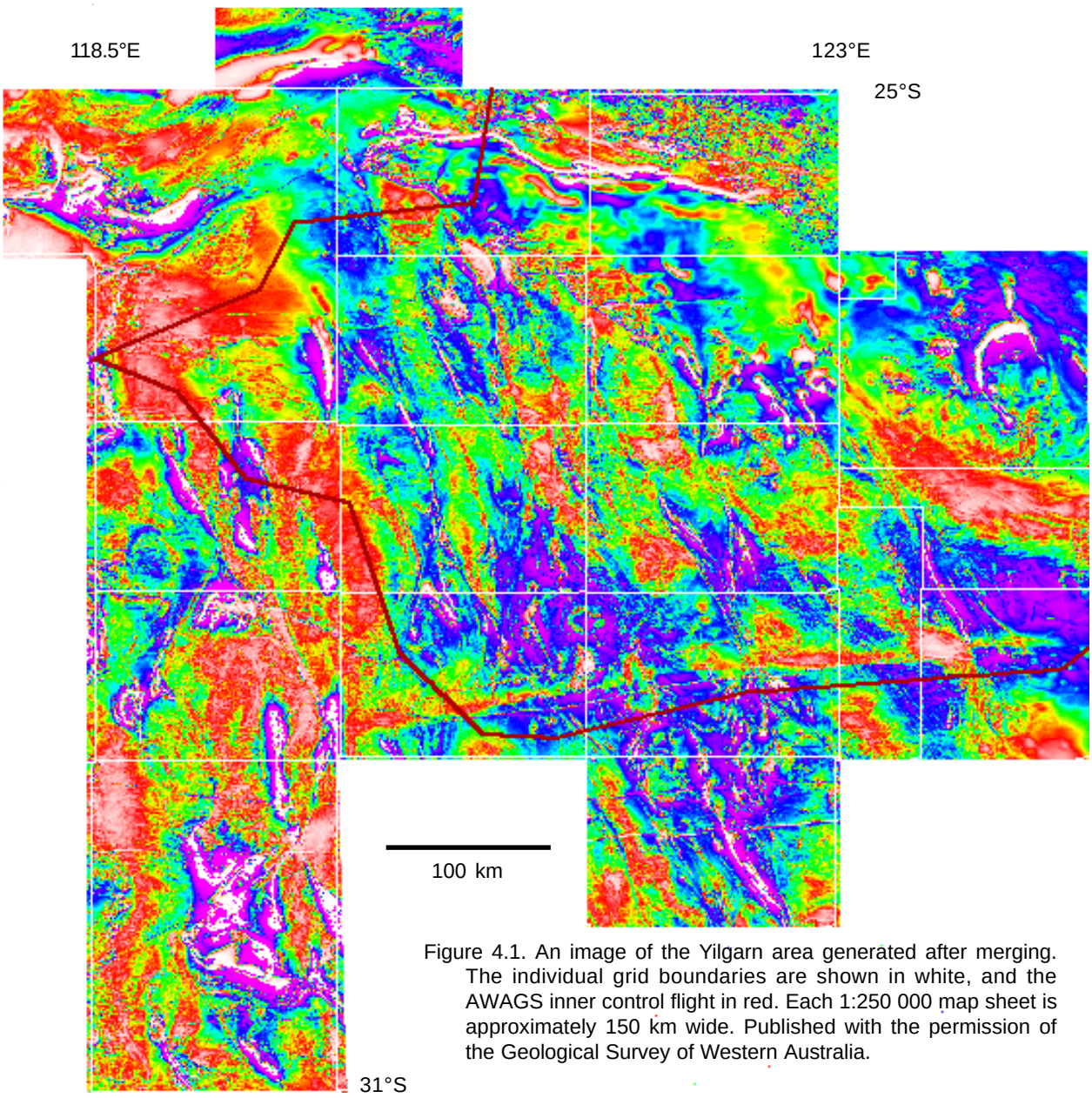

Figure 4.1. An image of the Yilgarn area generated after merging. The individual grid boundaries are shown in white, and the AWAGS inner control flight in red. Each 1:250 000 map sheet is approximately 150 km wide. Published with the permission of the Geological Survey of Western Australia.

data are lightly smoothed using a three-point running average filter to remove excessive high frequency values, and for ease of plotting the mean of each dataset is removed. High frequencies show up as noise in the comparison, which is concerned with the longer wavelength information. There will always be some mismatch in the higher frequency components due to differences in both TMI and navigation sampling resolutions of the datasets.

Test Areas and Results

Several areas across Australia are available for testing against the control traverses. The aeromagnetic survey data range in quality from poor to very high, and in coverage from small (a 1:250 000 map sheet area) to large (the whole of a state). This section describes the results obtained from a few representative areas.

1. The Yilgarn Area of Western Australia

A significantly sized area in the Western Australian Yilgarn Province is covered by recent, semi-detailed airborne magnetic data. Its approximate boundaries are 118.5° to 124.5° E and 25° to 31° S. This area is ideal as a first test of the gridmerging process, as it covers several 1:250 000 map sheet areas, is composed of data from several episodes of acquisition by different organisations, and also overlaps hundreds of kilometres of the inner circle of the AWAGS control traverses.

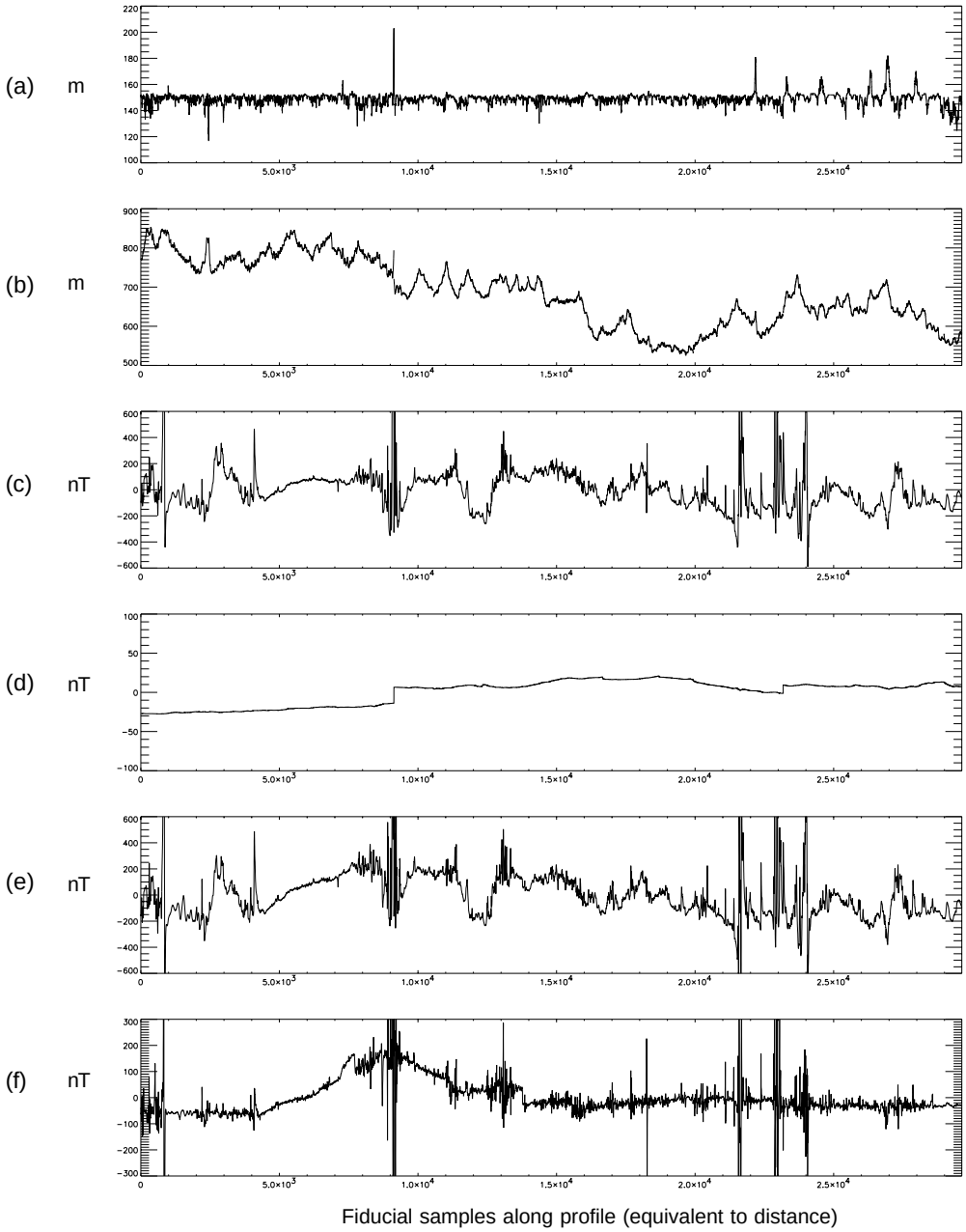

Figure 4.2. Comparison plots for the Yilgarn area of Western Australia. (a) The height of the aircraft above ground level (in metres). (b) The height of the aircraft above sea level (in metres). (c) The magnetic field residual from AWAGS flight. (d) The diurnal correction applied to (c). (e) The magnetic residual interpolated from the grid. (f) The difference between (c) and (e). Magnetic units are in nT. The width of the plot is approximately 1100 km.

Figure 4.1 shows an image of the merged data, and the path of the inner AWAGS control flight. For detailed information on the specifications of the individual surveys, see Richardson (2001).

The *Gridmerge* program has many options available to the operator for the combination of grid data; for full details see the Intrepid program manual. For the purposes of the tests, only three options are considered: DC adjustment of the data, DC adjustment then degree 1 adjustment, and supplying additional control data during the merging process. The program also reports the statistics of the merge, including the adjustments to each grid. These provide valuable information to the user in an attempt to obtain the best possible result.

The image in Figure 4.1 shows the result of merging the grids using only a DC shift for each grid. Superficially, the merged grid looks very good, with no obvious artefacts and long wavelength tilts.

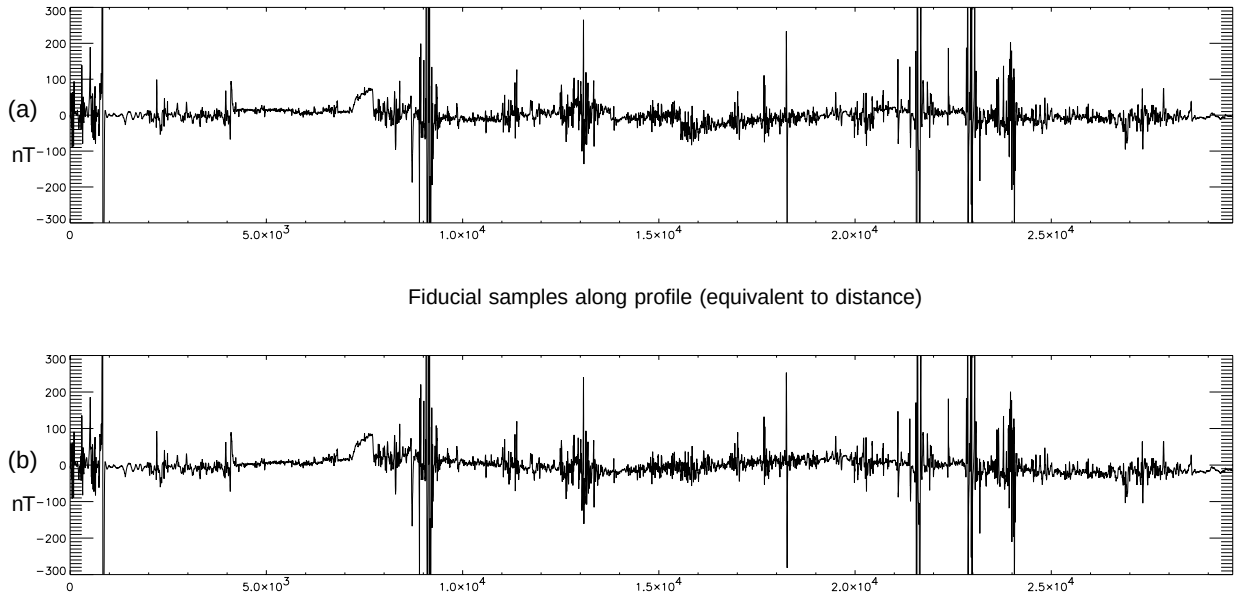

Figure 4.3. Results of the comparison of the Yilgarn area with the AWAGS inner flight after the tilt in the Glengarry grid has been corrected. (a) Degree 0 shift, (b) degree 0 shift and degree 1 tilt. X-axis units are fiducials; y-axis units are nT.

Figure 4.2 shows the results of the comparison. In theory, plot (f) should be a horizontal straight line. In practice, as mentioned previously, significant differences in the spatial high frequencies are to be expected, given that the magnetic grid is sampled at places not on the AWAGS flights, and interpolated. If these mismatches are discounted, then the comparison is reasonable except for the positive anomaly of about 200 nT on the left.

When the anomaly is related to the image in Figure 4.1, it occurs on that segment of the flight line that spans the Glengarry sheet, where the direction of flight changes from south-west to south-east. The peak of the anomaly is at the point of change of flight direction. Thus, it appears that this grid is tilted for some reason.

This conclusion has been confirmed independently using the Third-order dataset (see Chapter 5). In fact, the Third-order data have been used to define and remove a degree 1 surface from the Glengarry grid, and the new results of the comparison are displayed in Figure 4.3. The anomaly has now been removed, and the results are substantially improved. There are still long wavelength artefacts, but these are due to tilts in other grids.

It is interesting to speculate why the Glengarry grid should have an incorrect tilt. It is comprised of modern data, from which the correct IGRF should have been removed. The data were supplied to GSWA under contract, and it would be assumed made that the contract processor removed the appropriate IGRF. If this were not the case, then such a tilt could have been introduced. Alternatively, it could have been introduced during the levelling of the data, after IGRF removal; but it is less likely that it would have just been a degree 1 surface in this case, and not a higher order. Whatever the reason, as can be seen, correct IGRF removal is very important if long wavelength information is to be accurately portrayed in merges of magnetic data over large areas. Incorrect IGRF removal will probably be responsible for many spurious long wavelength components in areas of older, lower resolution data.

Tilts in the other grids are substantially less than that in Glengarry, and the option of degree 1 tilting in the *Gridmerge* program shows whether these tilts can be reduced automatically, rather than independently operating on the original grids.

Gridmerge has been run again merging the component grids using the option of allowing DC adjustment and also degree 1 adjustment, and the results are displayed in Figure 4.3(b). As can be seen, this produces a

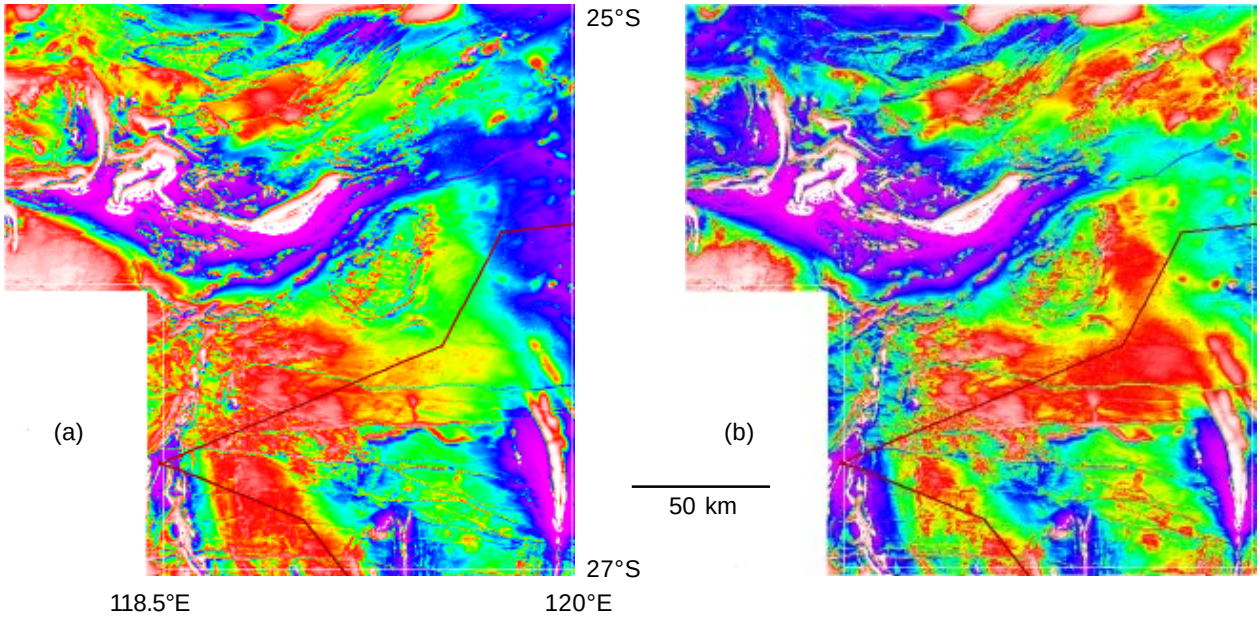

Figure 4.4. Images of the Peak Hill / Glengarry dataset (a) before, and (b) after the removal of a degree 1 surface. Published with the permission of the Geological Survey of Western Australia.

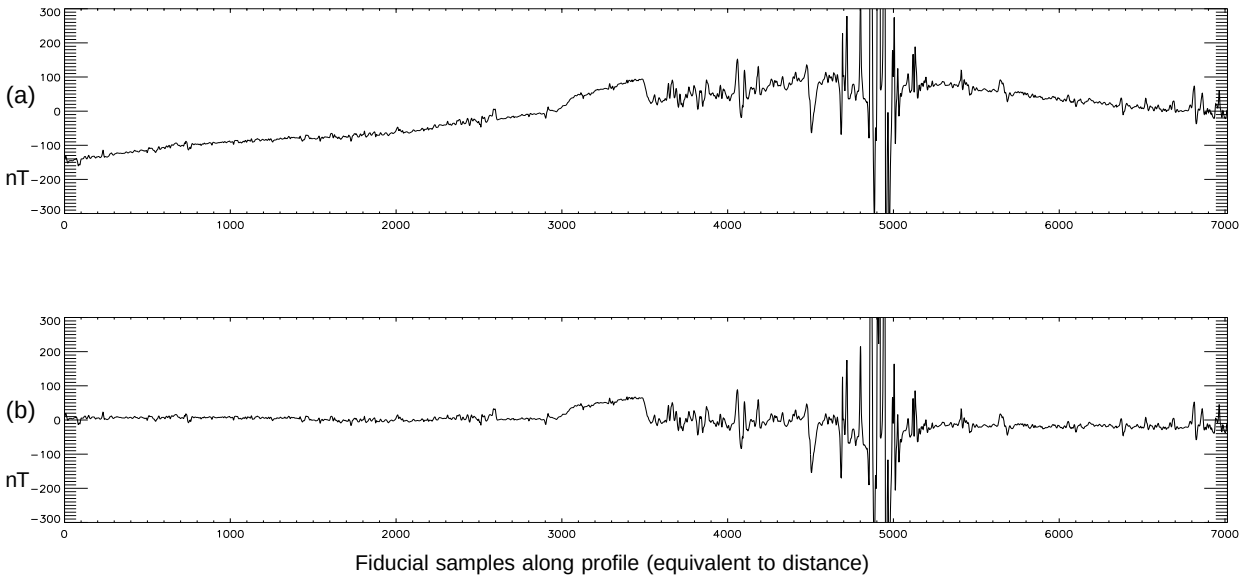

Figure 4.5. Differences between the Peak Hill / Glengarry data and the AWAGS inner control flight, (a) before, and (b) after the removal of a degree 1 surface. The width of the plot is approximately 270 km.

smoother result in that the discontinuities at the edges of the tilted grids are removed as the program has adjusted the tilts to match up the edges. However, if there is no control over the grids that are tilted by the program, the end result is not necessarily ideal, and in fact longer wavelengths could possibly be introduced into the final grid. This is discussed in more detail in Chapter 6, where the *Gridmerge* program is tested using model data.

2. *Peak Hill / Glengarry area of Western Australia*

The Peak Hill / Glengarry area of Western Australia is part of the area described above, and is shown in more detail in this section. The plane removal process is described in the next chapter. Figure 4.4(a) is a total magnetic intensity image of the original grid data, with the AWAGS control flight overlaid, and Figure 4.4(b) is a TMI image with the anomalous planar tilt removed from the data. These images emphasise how important such gradients can be in interpreting the long wavlengths in aeromagnetic data.

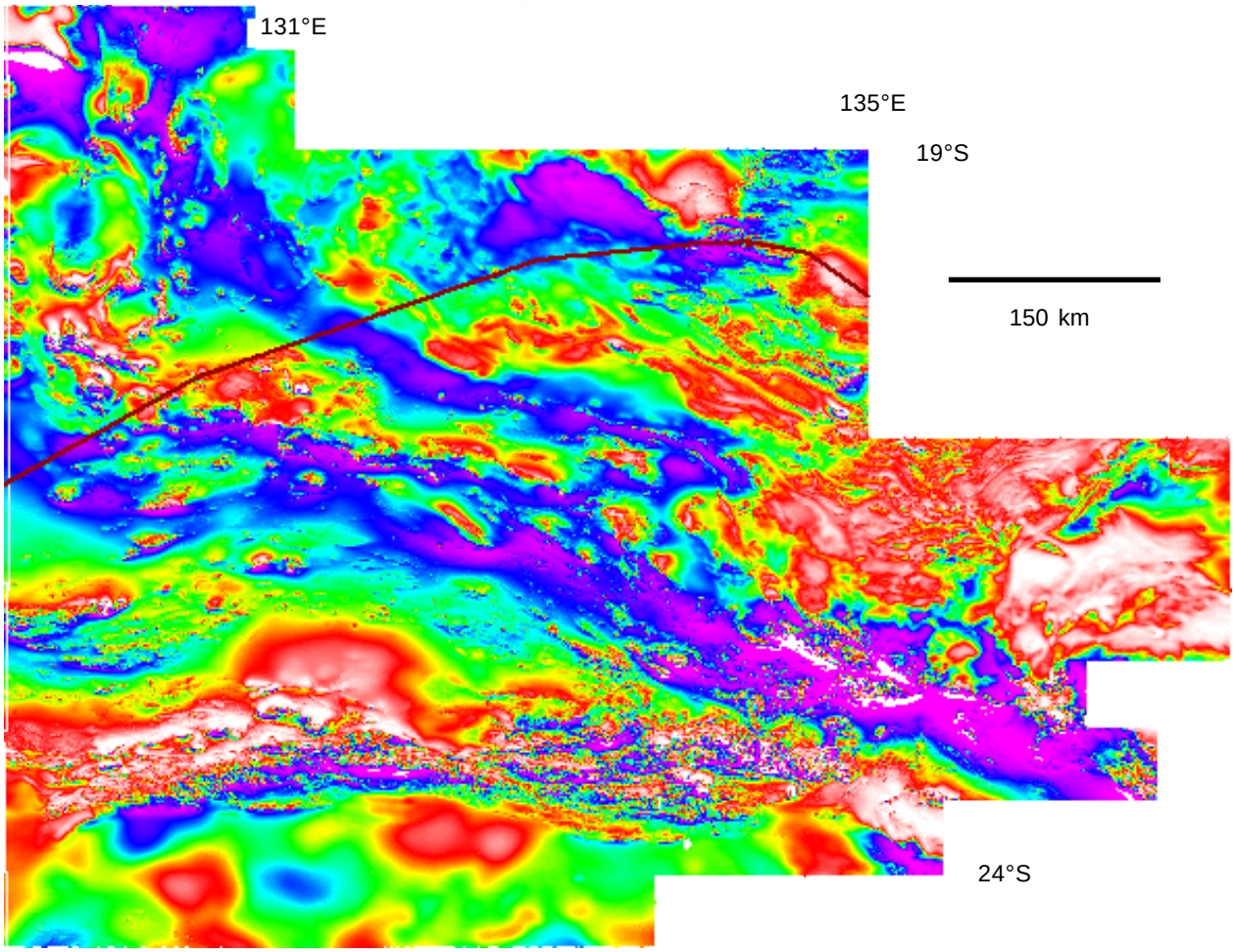

Figure 4.6. A TMI image of the Tanami – Arunta area of the Northern Territory, covering some of the AGSO / NTGS North Australian Craton project area. The AWAGS control flight is shown spanning the northern part of the area. Published with the permission of the Northern Territory Geological Survey.

Figure 4.5 provides the profile comparison along the AWAGS flight line, before and after removal of the tilt. It is observed that the grid and the AWAGS traverse data have a difference between records 3000 and 3500 which cannot be explained by slight sample location misplacements. It is of a longer wavelength than these, and represents a fundamental difference between the two datasets. At present it is unexplained. One of the datasets is in error, causing this difference.

3. Tanami – Arunta Area

Airborne magnetic data covering the tanami – Arunta area of the Northern Territory have been compiled into a single grid as part of the AGSO / NT Geological Survey North Australian Craton Project.

An image of the area, and the AWAGS control flight intersecting it, is shown in Figure 4.6. Unfortunately, only a small portion is crossed by the flight, mainly in an east–west direction.

Figure 4.7 shows the profile plots, and it can be observed that for the portion of the line available, the comparison is extremely good, with very small differences, and a virtually horizontal difference plot.

4. Curnamona Region of South Australia and New South Wales

Modern data for this region were acquired under the Broken Hill Exploration Initiative (BHEI) program, which involved the governments of South Australia, New South Wales and the Commonwealth collaborating under the auspices of the National Geoscience Mapping Accord (NGMA). This Commonwealth/State collaboration still continues, under the National Geoscience Accord (NGA).

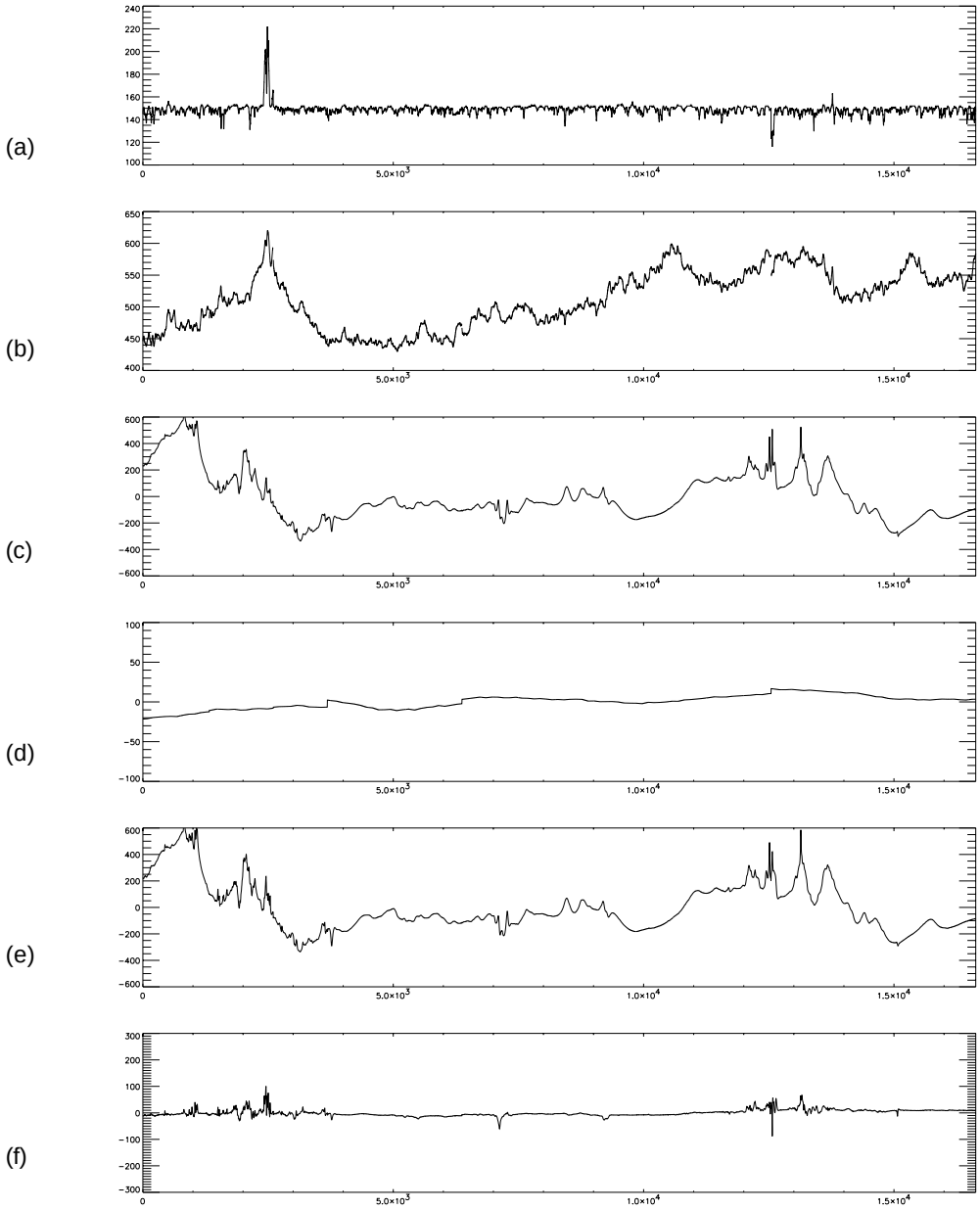

Figure 4.7. Comparison between the grid data (nT) and the AWAGS control flight for the Northern Territory data shown in Figure 4.6. (a) The height of the aircraft above ground level (in metres). (b) The height of the aircraft above sea level (in metres). (c) The magnetic field residual from AWAGS flight. (d) The diurnal correction applied to (c). (e) The magnetic residual interpolated from the grid. (f) The difference between (c) and (e). The width of the plot is approximately 650 km.

The recent data acquisition program commenced in 1995, with AGSO acquiring data with its own aircraft, and South Australia contracting data acquisition under the South Australian Exploration Initiative (SAEI) umbrella, New South Wales under the Discovery 2000 umbrella. Regional data surrounding this region were also available, mainly BMR and public domain company data. Full specifications of all the surveys can be found in Richardson (2001). Images and geographic information of the region are contained in Milligan *et al.* (2000).

The TMI grid data for this region were merged several years ago using an older technology than the new *Gridmerge* program. Intrepid *Gridstitch* software was used, which basically allows two overlapping grids to be merged at a time, using the statistics of the overlapping region to define polynomials for adjusting one of the grids. As mentioned in Chapter 1, this type of process provides very poor control of long wavelength information, and there is a tendency for errors to be propagated across a whole region.

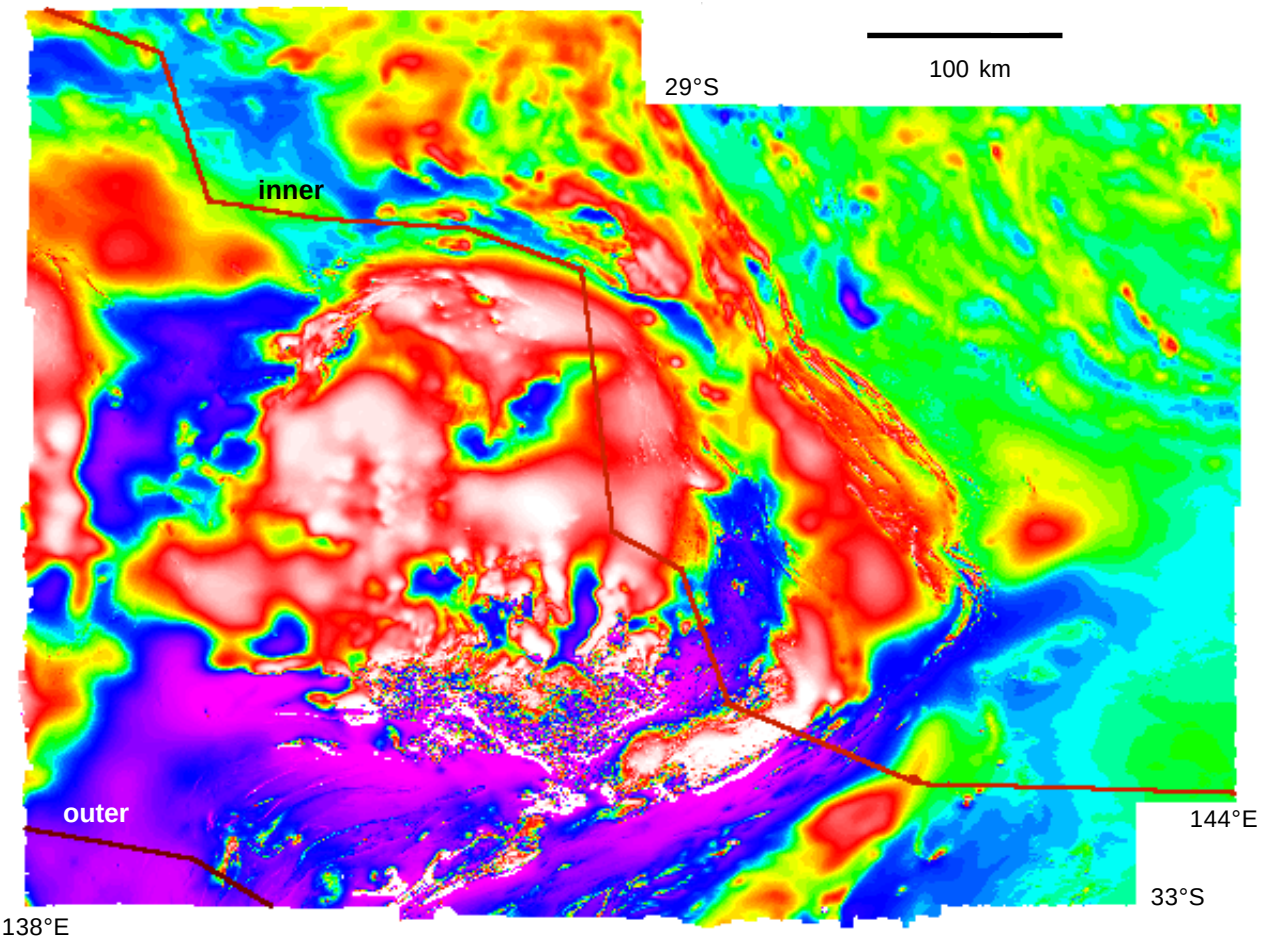

Figure 4.8. A TMI image of the Curnamona Region of South Australia and New South Wales, covering the Broken Hill Exploration Initiative area. The AWAGS control flights are shown crossing the area. Refer to Milligan (1999) and Milligan *et al.*, (2000) for published images. Published with the permissions of Primary Industries and Resources, South Australia and the Geological Survey of New South Wales

In the *Gridstitch* merging process, the highest quality central data were merged first, and the surrounding lower-quality regional data were added as the last step. Only degree 0 (DC shift) or degree 1 polynomials were used, in an attempt to reduce contamination of the longer wavelengths to a minimum while maintaining a high degree of matching between the datasets. Diurnally corrected AWAGS flight data were not available when these data were merged, and they now provide an interesting comparison with this older dataset.

Figure 4.8 is a TMI image of the area, with both the inner and outer AWAGS control flights superimposed, and Figure 4.9 provides the standard comparison plots. These plots indicate a remarkably good agreement between the grid and the AWAGS flights, with only very small regional gradients and along-line differences. This highlights the ease with which modern high-quality data can be merged, compared to older, more regional data which are much less accurate.

5. Magnetic Anomaly Map of Western Australia

The final grid to be compared is that formed by merging grids from all the projects that cover Western Australia. An image of the Magnetic Anomaly Map of Western Australia has been published jointly by AGSO and the Geological Survey of Western Australia (Mackey *et al*., 1999) using grids that were merged with an early implementation of the *Gridmerge* software. This early version will be compared here, and also three others merged using the most up-to-date software.

Figure 4.10 shows our final image of the area with the survey outlines superimposed in white, and the AWAGS control flight lines in other colours, depending upon the particular day of acquisition.

For the comparison of this large region, the profiles to be compared are low-pass filtered before they are plotted and before the various statistics are calculated.

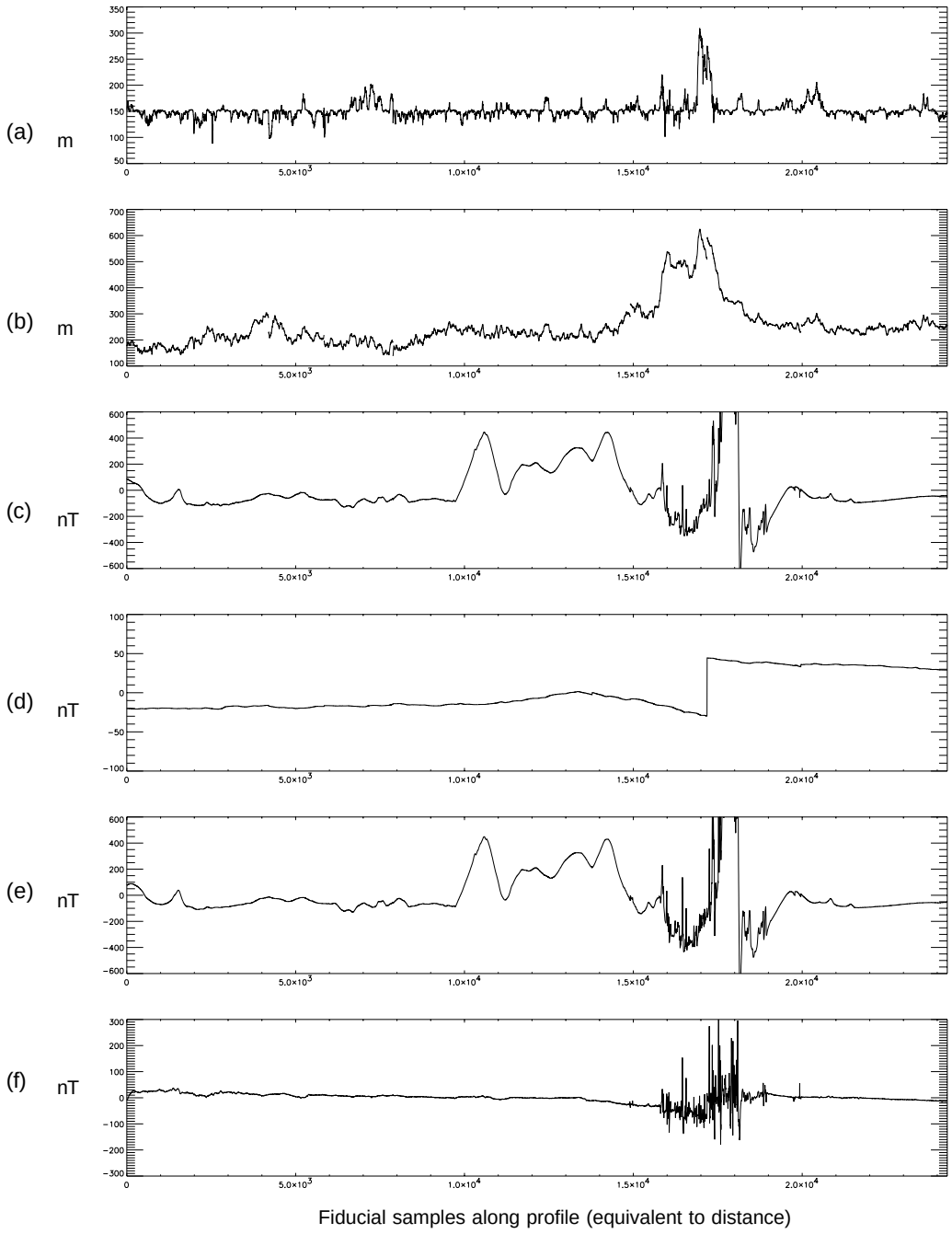

Figure 4.9. Comparison plots for the inner AWAGS control flight line across the Curnamona Region, as shown on the image of Figure 4.8. Refer to Figure 4.7 for a detailed description of each graph. The step in the diurnal trace (d) represents the difference in the diurnal correction between two successive flights. The width of the plot is approximately 835 km.

Comparison plots for the early grid of Western Australia are shown in Figure 4.11. The important traces to consider are the filtered difference plots for both the inner and outer AWAGS flights. It can be observed that there are mis-matches of hundreds of nT in the long wavelengths, with a particularly severe gradient towards the right hand side of the plot of the outer flights, which represents the south-eastern section of the grid of Western Australia.

An early implementation of *Gridmerge* was used to combine this version of the Western Australian data — the latest implementation is more robust, and this type of artefact is very unlikely to occur.

Another way of showing the correlation between the two datasets is to plot one against the other, as shown in Figure 4.12. The profiles were both low-pass filtered before this plot was generated. It shows very clearly how different sections of the profiles compare — they tend to fall into parallel groupings, and the region to the

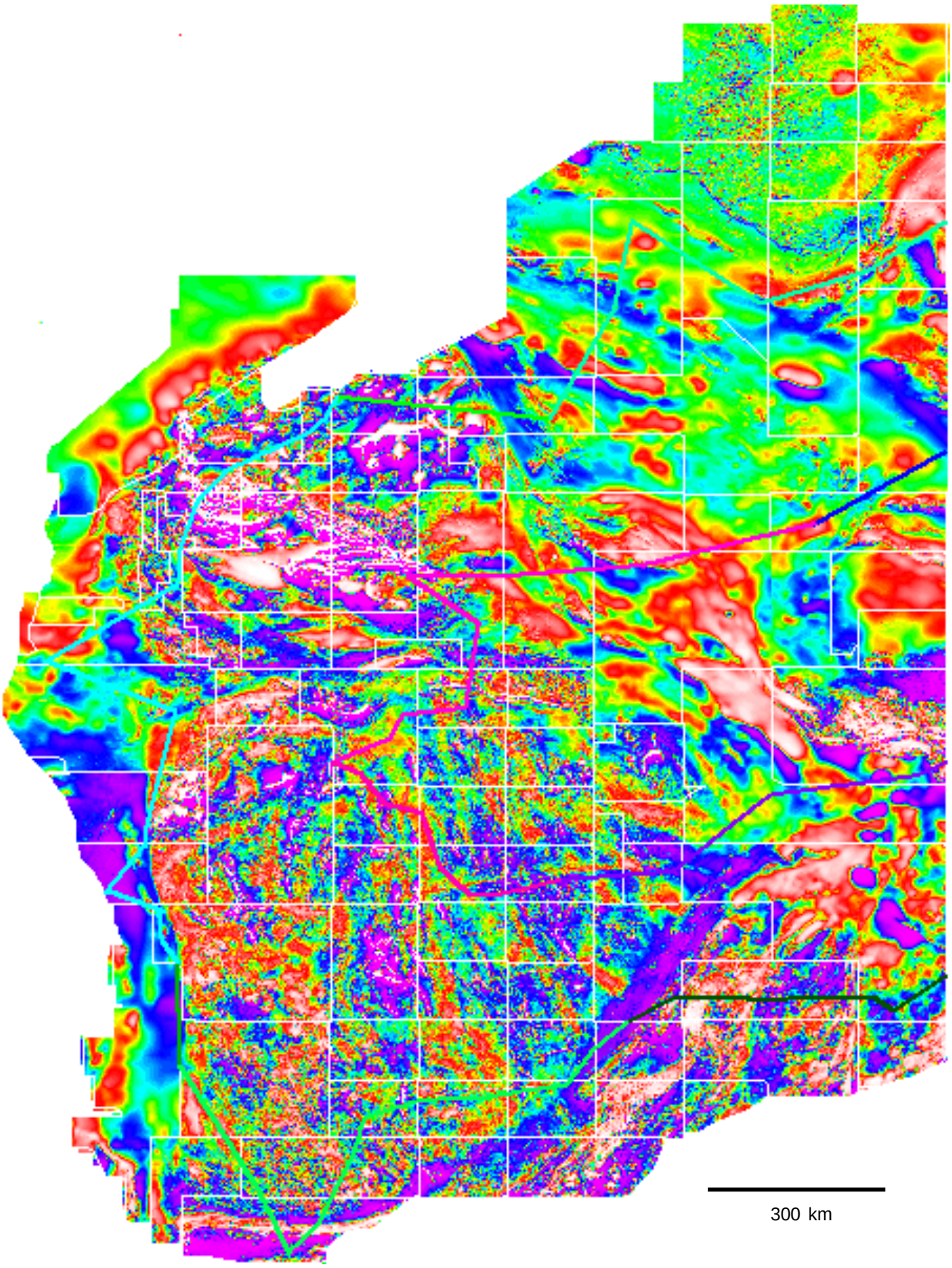

Figure 4.10. An image of the TMI of Western Australia, with survey outlines and AWAGS control flights superimposed. The different colours of the flights refer to separate acquisition days. Published with the permission of the Geological Survey of Western Australia.

south-east is now particularly prominent (right-hand side of figure). This plot indicates that short sections of the grid compare favourably, but when they are all merged together, there are major disparities between the merged sections. The correlation coefficient and standard deviation of the differences are provided, and will be compared with those from the next sets of data. Note that the correlation coefficient is very high, as it should be — the two datasets are highly correlated, but in theory they should be perfectly correlated.

The next result of *Gridmerge* (using the latest version) to be compared is that generated by using only a DC shift to all the grids. Results are shown in Figure 4.13, and the correlation plot in Figure 4.14. These plots show that although there are still major areas of poor match, the result is much better than in the previous example. Note now that the correlation coefficient has increased to 0.9, and the standard deviation of the differences has fallen to 73.5 nT.

Figures 4.15 and 4.16 take the process one step further, and allow the grids to be tilted to degree 1 as the final step in the merging process. However, no base grids are defined, and the tilting process is unconstrained by the operator as to which grids are tilted. As can be seen, there is again an increase in the correlation coefficient and a decrease in the standard deviation, but there are still large differences in the final result. The tilting has had a major effect on the poor match to the right of the plot. In general, however, tilting will not significantly improve the long wavelength information if done in an unconstrained fashion, as there is a danger that grids which do not require tilting are tilted, and further errors are introduced. The correlation coefficient has now been increased to 0.916, and the standard deviation decreased to 66.15.

The final grid to be compared has been generated using the AWAGS flights themselves as a control in the gridmerging process. The grids which overlap with the flights are set to the DC level of the flights. This is an option that has been built into the *Gridmerge* program to allow such control where high-quality datasets exist. Ideally, all gridmerge operations should use a standard control set of values, but these do not exist in high quality for the whole of Australia. The topic is further discussed in Chapter 5.

As might be expected, this implementation of the merge provides the best fit of all, with a correlation coefficient of 0.969 and a standard deviation of 37.5. Results for the outer AWAGS flights are summarised in Figures 4.17 and 4.18.

The correlation coefficients and standard deviations for each of the four merged datasets are summarised in the following table

Method	Correlation Coefficient	Standard Deviation
Early grid	0.857	97.68
DC shift only	0.900	73.5
DC shift & tilt	0.916	66.15
DC shift, tilt & ref.	0.9688	37.5

Summary

The *Gridmerge* program significantly improves the quality of merged datasets in terms of the accuracy of long wavelength information, particularly when compared to older technology applied to a variety of grids acquired over a large time span with differing quality of specifications.

Best results are obtained when there are accurate control values with which to constrain the merging process. The results presented in this chapter have, by necessity, only compared the merged grids to the AWAGS traverses. There is no indication of how well the merging process works for areas other than those covered by the traverses. Chapter 6 attempts to address this, by comparing merged areas with the Third-order dataset.

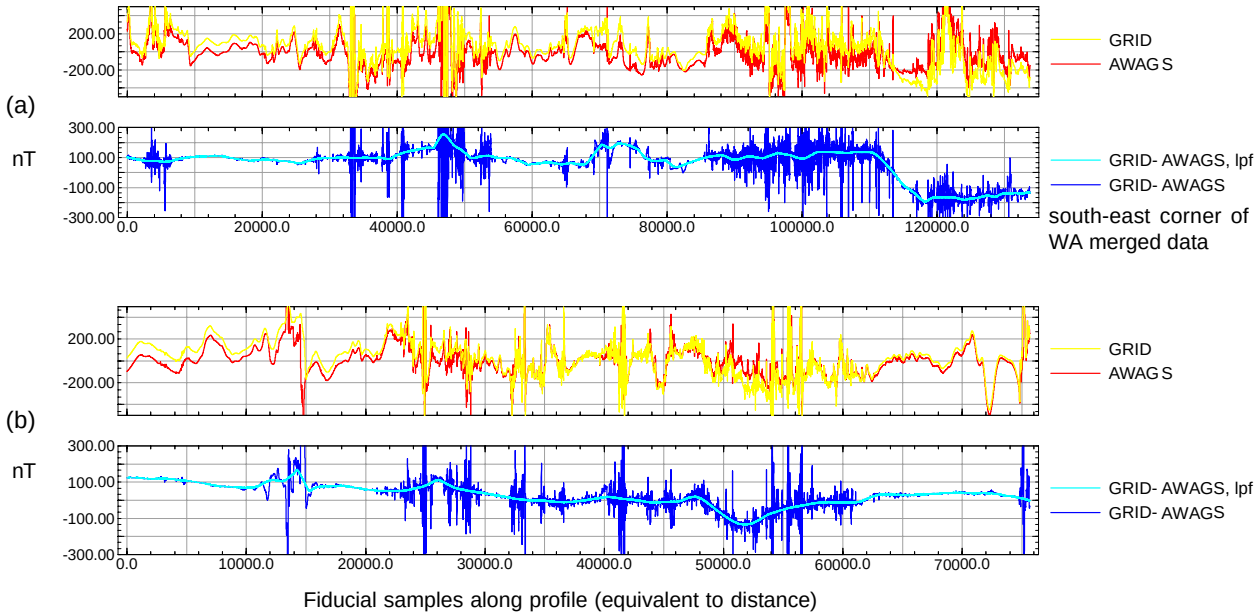

Figure 4.11. Comparison plots for (a) the outer AWAGS flights, and (b) the inner flights with the early TMI merged grid of Western Australia. The difference plot has been non-linearly low-pass filtered to emphasise the longer wavelength mismatch. The width of (a) is approx. 4,500 km, the width of (b) is approx. 2,500 km.

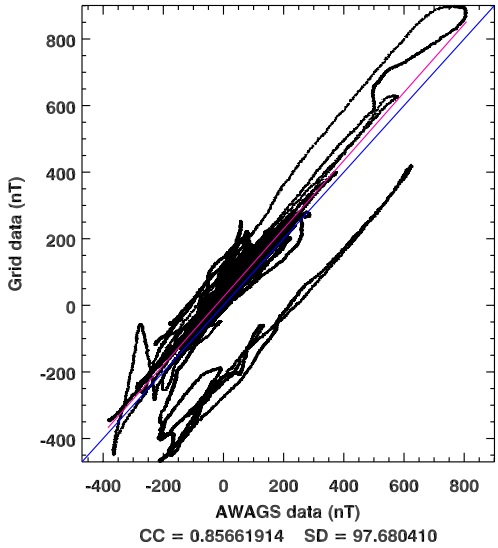

Figure 4.12. Correlation plot between the AWAGS outer flights and the early grid merge of Western Australia

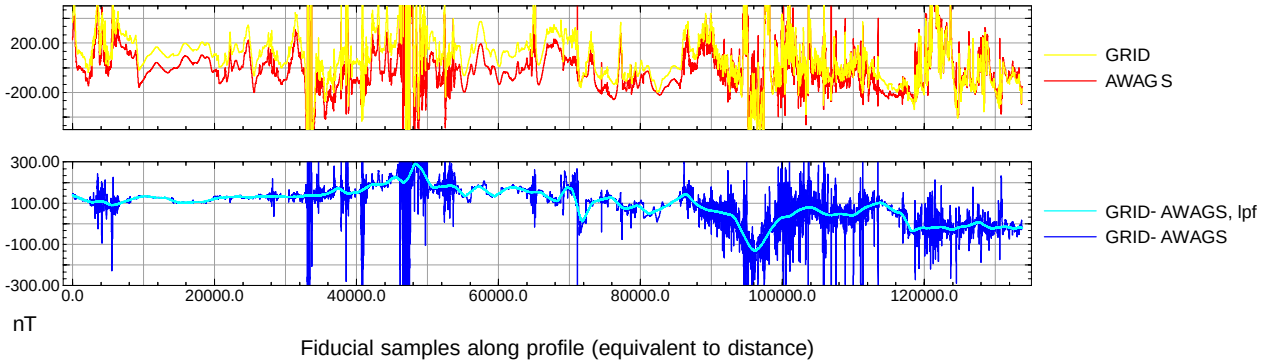

Figure 4.13. Comparison plots for the outer AWAGS flights and the TMI grid of Western Australia, merged using only DC shifting of the individual grids

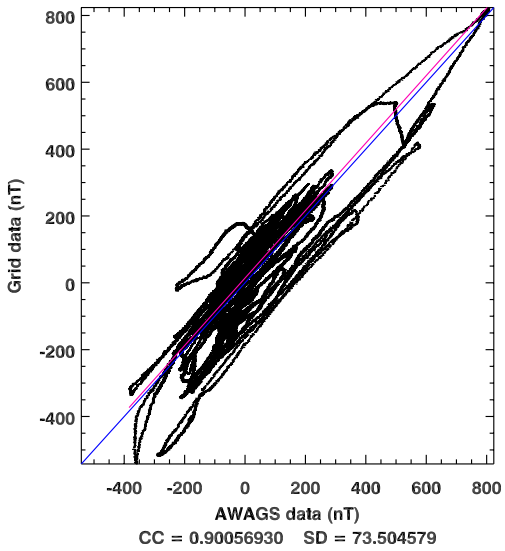

Figure 4.14. Correlation plot between AWAGS outer flights and the DC shifted grid merge of Western Australia

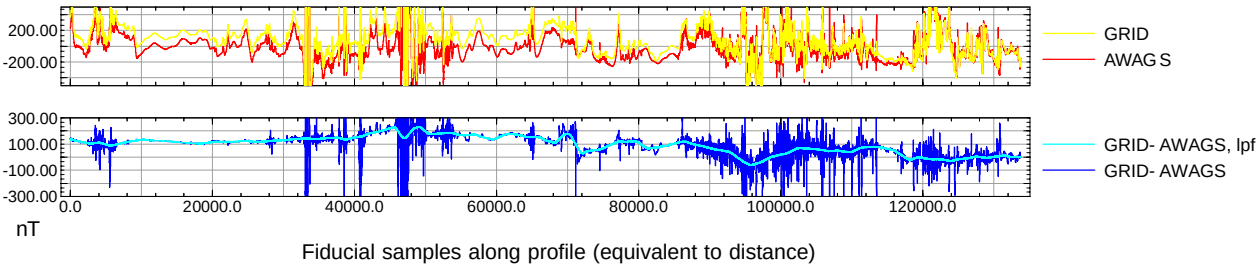

Figure 4.15. Comparison plots for the outer AWAGS flights and the TMI grid of Western Australia, merged using DC shifting and then tilting of the individual grids

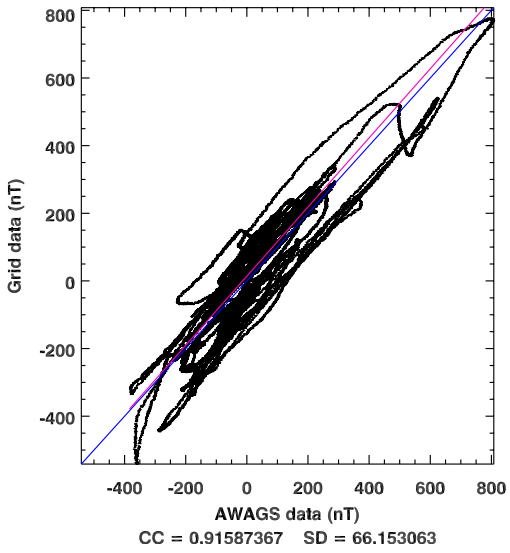

Figure 4.16. Correlation plot between AWAGS outer flights and the DC shifted, tilted grid merge of Western Australia

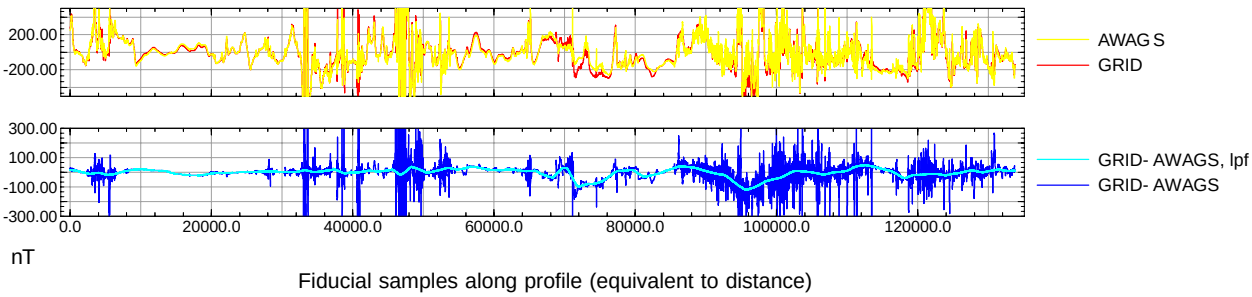

Figure 4.17. Comparison plots for the outer AWAGS flights and the TMI grid of Western Australia, merged using DC shifting and tilting, with AWAGS fligh control as well

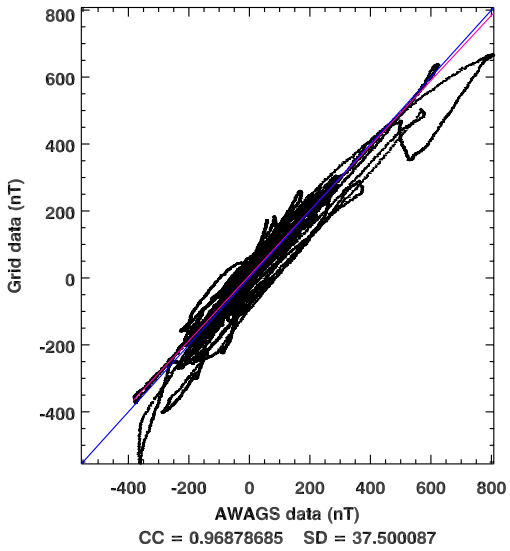

Figure 4.18. Correlation plot between AWAGS outer flights and the DC shifted, tilted grid merge of Western Australia

5. THIRD-ORDER COMPARISONS

Introduction

The Third-order dataset has been documented in Chapter 3. Although not as precise as the AWAGS control traverses, it has the one major advantage in that it provides an independent distribution of total magnetic intensity (TMI) data across the whole Australian continent in a semi-random fashion. The shortcomings of this distribution, already mentioned, make it very difficult to grid the data into a surface which is not biased by sampling problems (aliasing). However, this chapter explores possible ways in which the Third-order may be used to help validate merged airborne TMI grids.

Method

Data are interpolated from the TMI grid under consideration at the Third Order positions. As the positional errors in the Third-order data are potentially large, the horizontal gradients of the grid are calculated using the grid cells closest to the interpolated position. Data are then rejected if the maximum horizontal gradient at this point exceeds 10 nT per cell spacing. A second rejection criteria used is the magnitude of the difference between the Third-order data and the interpolated grid value. If this difference exceeds ±150 nT, then the data point is not used.

As mentioned in Chapter 3, both raw and corrected Third-order data can be compared with grid data, and various results plotted out. Also estimated is the best fitting plane to the differences between the datasets. If there are enough samples across the area under consideration for this to be statistically meaningful, given the nature of the errors in the Third-order dataset, then a check can be made to determine whether the processing of the grid under test has adequately removed the IGRF component.

Test Areas and Results

1. Peak Hill / Glengarry Area of Westen Australia

As mentioned in Chapter 4, this area was found from the AWAGS control flights across it to have an erroneous tilt. Therefore this comparison provides a useful starting point with the Third-order data. It should be pointed out, however, that as this grid covers an area of just two 1:250 000 map sheets, it is pushing the limits of the Third-order data to extract a valid comparison.

Figure 5.1 shows a histogram-equalised TMI image of the area with the Third-order data acquisition positions superimposed as black stars.

It is observed that the Third-order sample locations across this area were along roads or tracks, which highlights some of the sampling issues involved when such sample sites are superimposed on a high-resolution image. For example, the line of sites trending north-north-east in the western area appear to follow a linear magnetic high anomaly. This could be because the rocks which form the anomaly also form a topographic ridge, with the road along its crest. Alternately, the road could follow a valley which has been preferentially weathered in the anomaly forming rocks. Either way, this sort of sampling seriously biases the data.

Also note that there are high gradient areas in the data, close to the centre of the image. Data are not used from these sites because of the large magnetic gradients, as explained above.

Figures 5.2(a),(b) are images of the area derived from the grid data and the Third-order data respectively, but gridding only those data at the Third-order sites which remain after the selection process. A linear stretch has

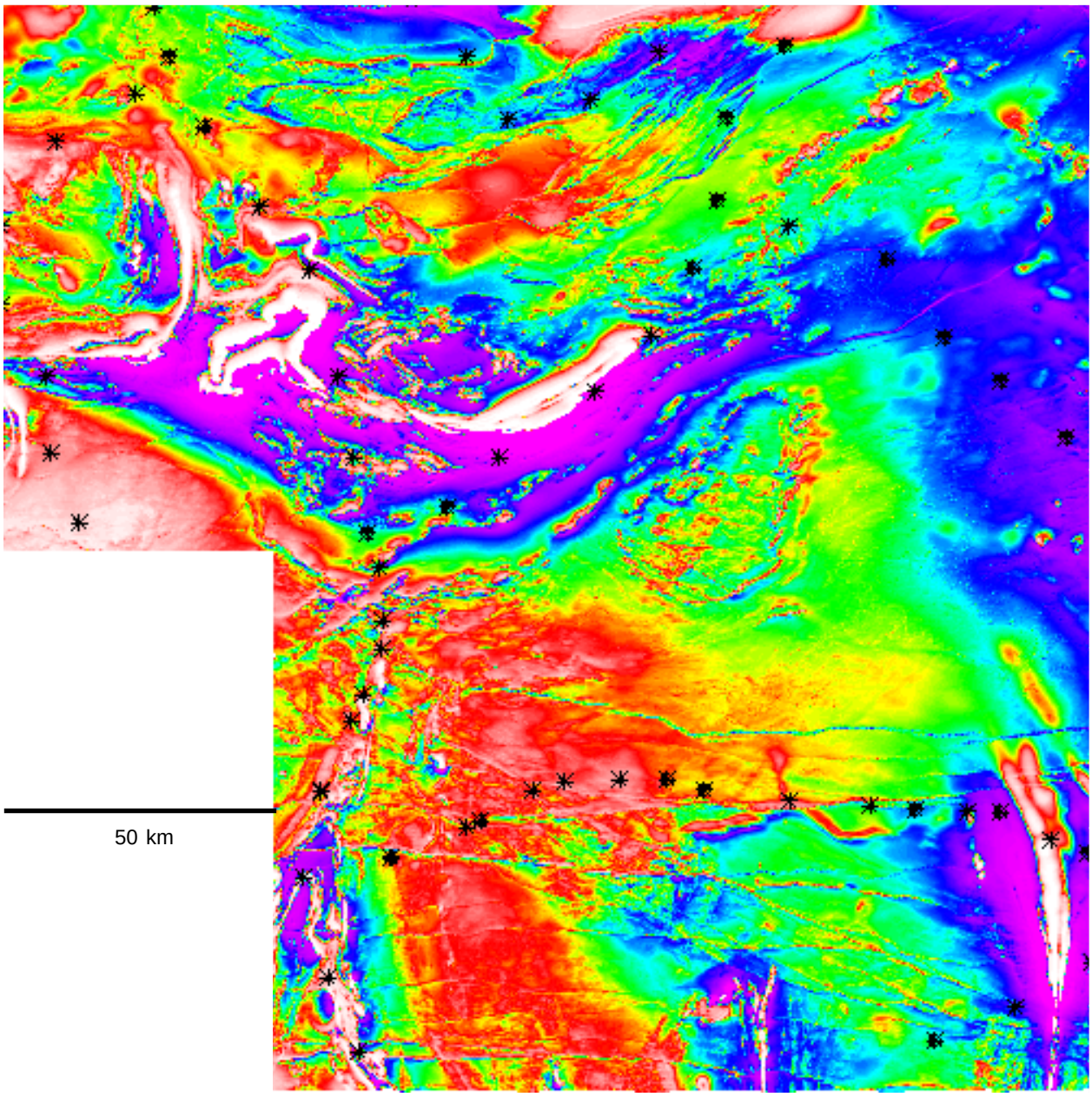

Figure 5.1. Histogram equalised image of the Peak Hill / Glengarry data, with Third-order sample sites as black stars. Published with the permission of the Geological Survey of Western Australia.

been applied in the generation of these images. As can be observed, even with so few data points, there is a difference in east–west gradient between the data, with the Peak Hill / Glengarry grid data high in the west compared to the east, while the Third-order data are higher in the east.

The degree of correlation between the two datasets is shown in Figure 5.3. While a straight line provides a reasonable fit to the data, there is a scatter of tens to hundreds of nT, which renders the data suitable only for a crude comparison.

The images in Figure 5.4 display a degree 1 surface fitted to the two datasets in a least-squares sense. Again, the image on the left is derived from the Peak Hill / Glengarry data, and the image on the right from the Third-order data. The differences in the tilts of the grids are obvious, and reinforce the comparison obtained from the AWAGS control flight data.

The magnitude of the tilt in the Peak hill / Glengarry grid data is large: –167 nT / degree in the west–east direction (–39 nT / degree south–north), compared with the Third-order data of –33 nT / degree west–east (–19 nT / degree south–north). There is very little difference between using Third-order data that have been

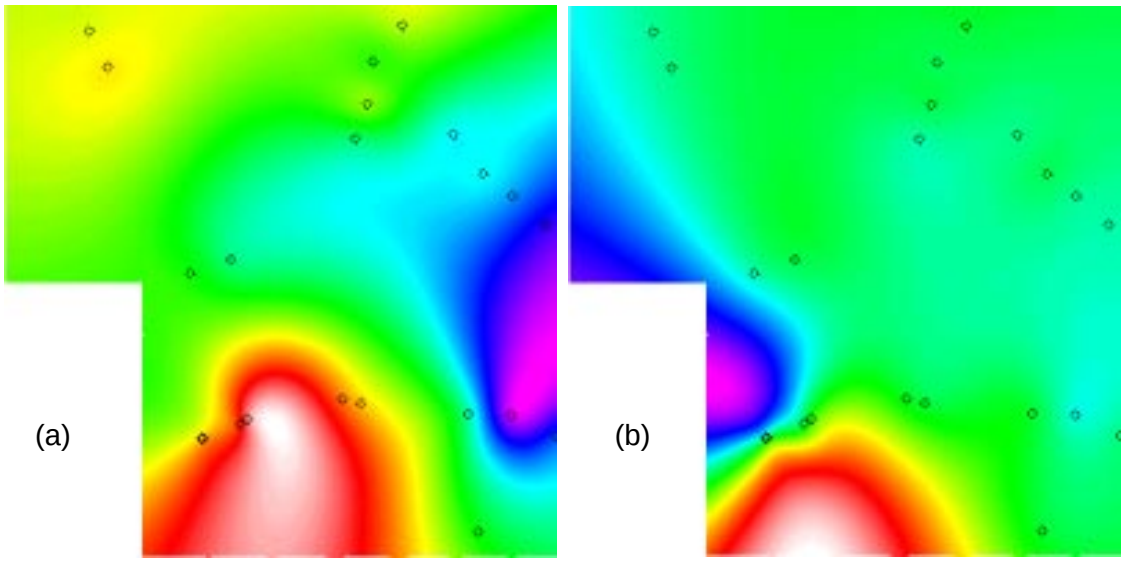

Figure 5.2. Image (a) is derived from the Peak / Glengarry airborne data, while image (b) is derived from the Third-order data

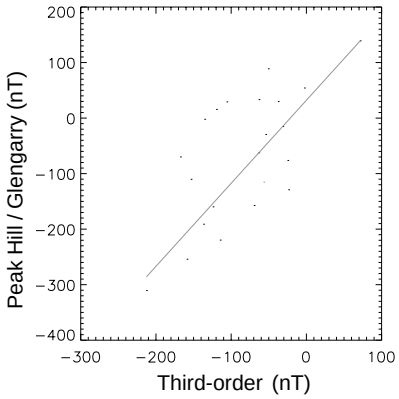

Figure 5.3. The correlation between the Third-order data (x-axis) and the Peak Hill / Glengarry data (y-axis)

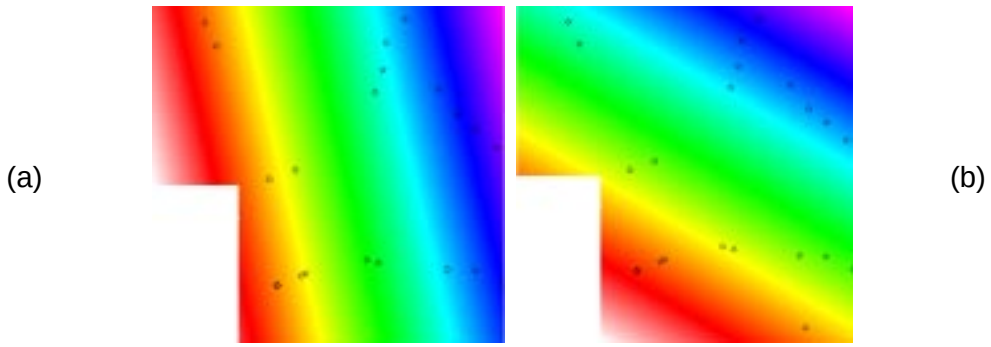

Figure 5.4. Images of a degree 1 surface fitted to (a) the Peak Hill / Glengarry data, and (b) Third-order data

diurnally corrected, and using those which have not been corrected.

2. Arunta – Tanami area, Northern Territory

The grid for this area is now compared with the Third-order data. In Chapter 4 it was seen that the comparison with the AWAGS control flights was favourable, but there was only a small portion of flights which overlapped the grid.

Figure 5.5 shows a histogram equalised image of the data with the Third-order sample points overlaid. As the area is much larger, and only of moderate relief, a much better statistical sample can be obtained than with the Peak Hill / Glengarry comparison above. The Third-order samples are a mixture of those acquired along roads and the helicopter survey which sampled a regular grid (refer to Chapter 3). Hence, the sampling is less biased than in the previous example, although one of the roads appears to follow a zone of magnetic low.
In Figure 5.6 the data at the Third-order sample sites are plotted against record number in the Third-order database (this equates to time of acquisition), together with the equivalent grid data, and the differences between the two.

Third-order data correlate well with grid data, as can be seen by the similarity of the top two traces. Also, although the point-to-point differences are significant, there is no significant bias, and they average around

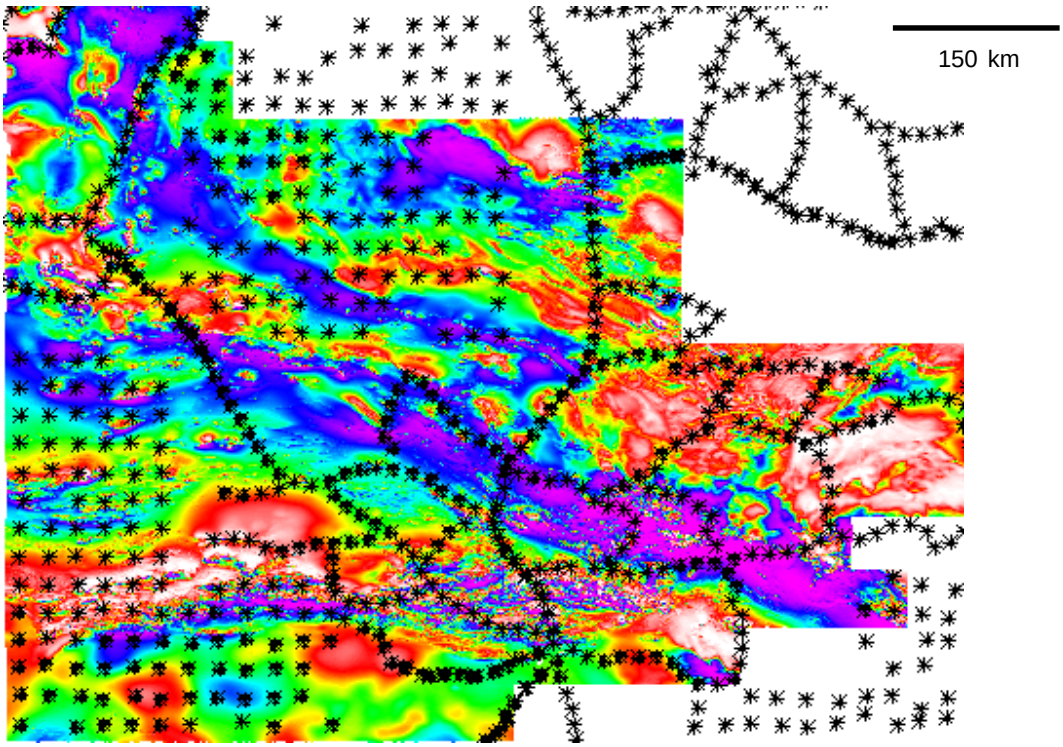

Figure 5.5. Histogram equalised image of the North Australian Craton TMI data, with the Third-order acquisition sites. Compare with Figure 4.6 for the AWAGS control traverse position. Published with the permission of the Northern Territory Geological Survey.

zero. The largest variations occur, where expected, in regions of large anomalies, where the horizontal gradients are large, leading to greater sampling errors.

Correlation plots of the Third-order data against the grid data are shown in Figure 5.7, with the best-fitting straight line. These indicate a high degree of correlation, and confirm the results obtained for this area from the AWAGS control traverses. There is again very little difference between using Third-order data that have been diurnally corrected, and using those which have not been corrected.

3. TMI Grid of Western Australia

The final dataset to be compared with the Third-order data is that of the grid of Western Australia, which has been merged from the individual project grids using DC shifts, tilting and the reference AWAGS control flights. An image of the area is shown in Figure 5.8, with the Third-order sites superimposed. These are the subset of sites left after culling by the conditions already mentioned. The density of data points in some

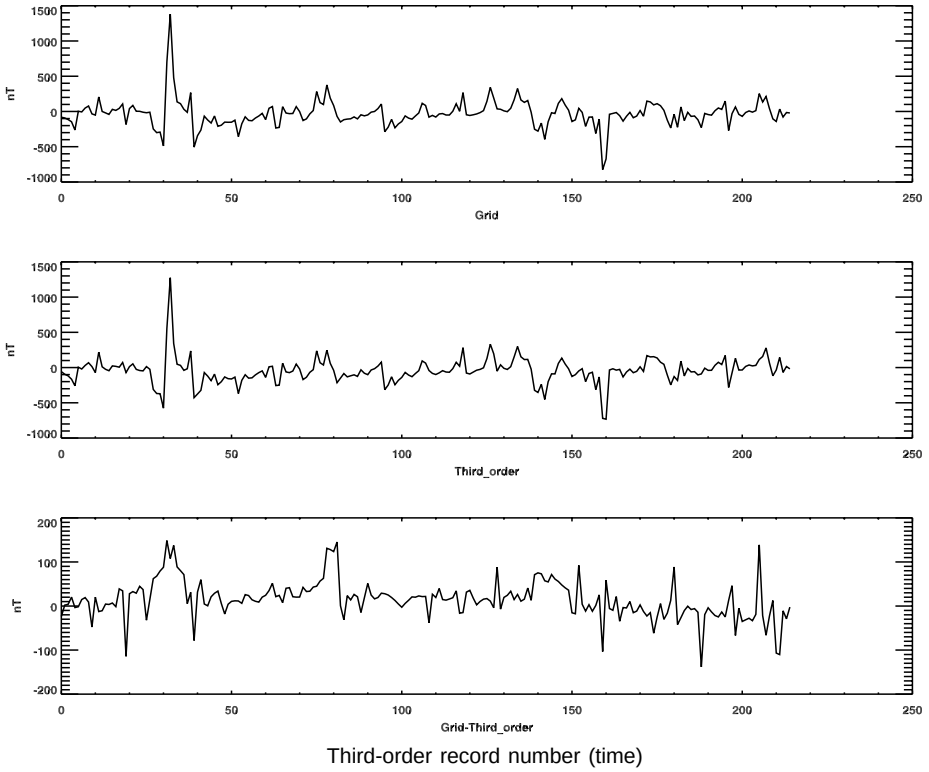

Figure 5.6. Grid data for the North Australian Craton project area of the Northern Territory (top), Third-order data, and their differences (bottom), plotted against the Third-order record number (which equates to time)

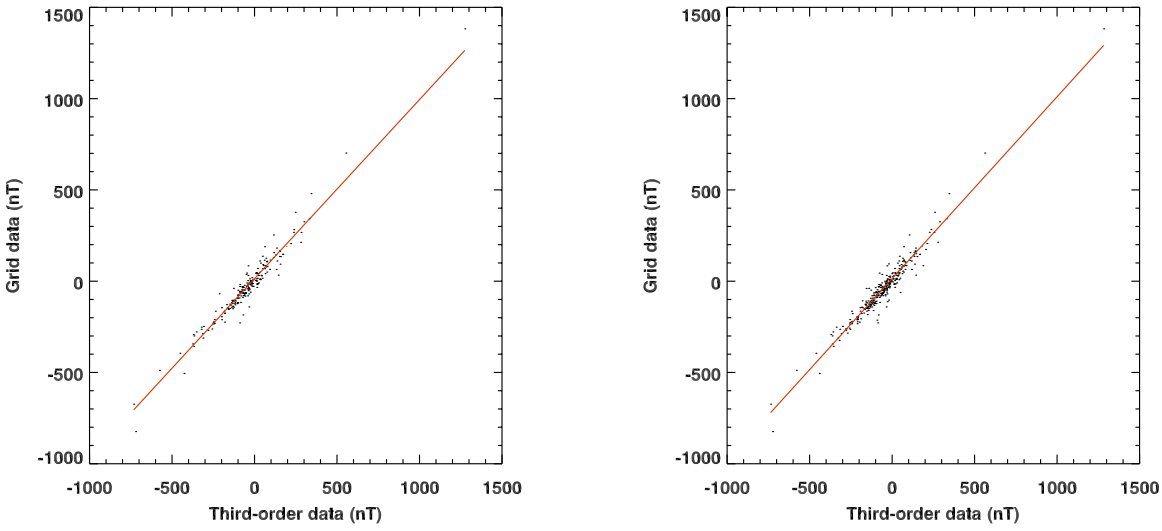

Figure 5.7. The correlation between the Third-order data and the NACP grid data, using diurnally corrected Third-order data (left) and Third-order uncorrected data (right)

regions, particularly the north-east and south-west, is significantly reduced.

Profiles of the data, and their differences, plotted against record number (time), are shown in Figure 5.9. The important plot is that of the differences; note the scale change from the two plots above. Although there is a significant scatter about the mean, there is no long period trend apparent in the differences, as would be expected if the appropriate IGRFs have been removed from both datasets.

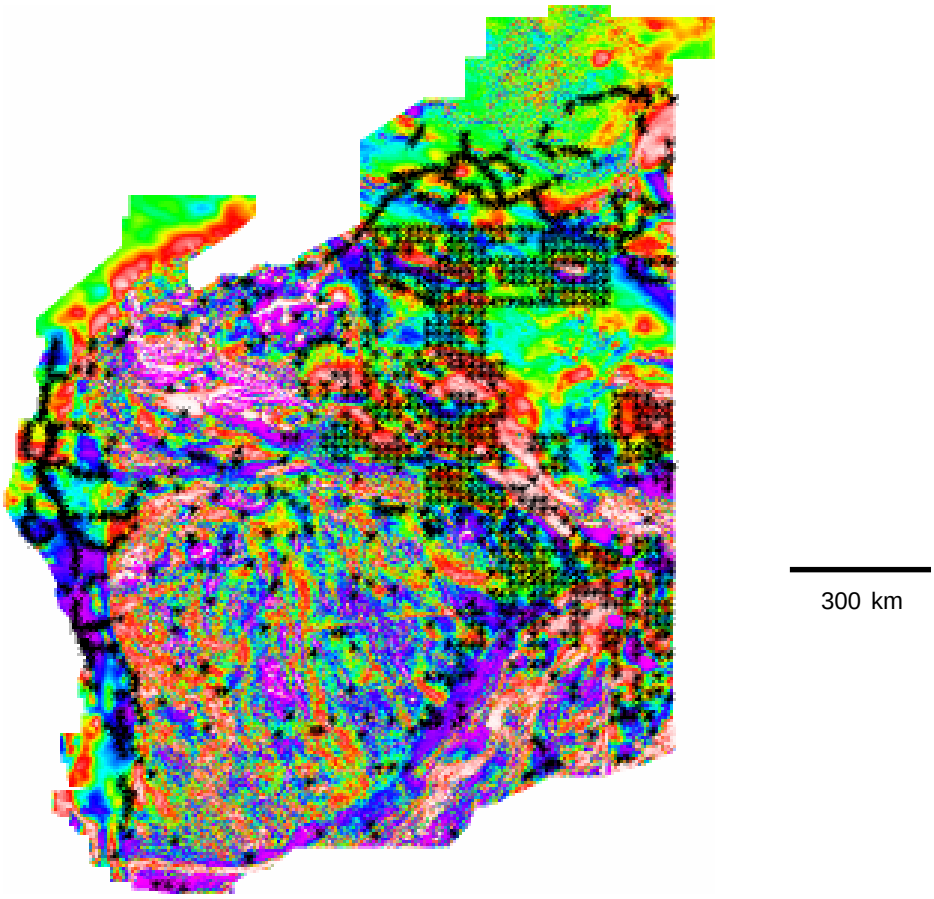

Figure 5.8. Histogram equalised image of the Western Australia TMI data, with the Third-order acquisition sites used in the comparison

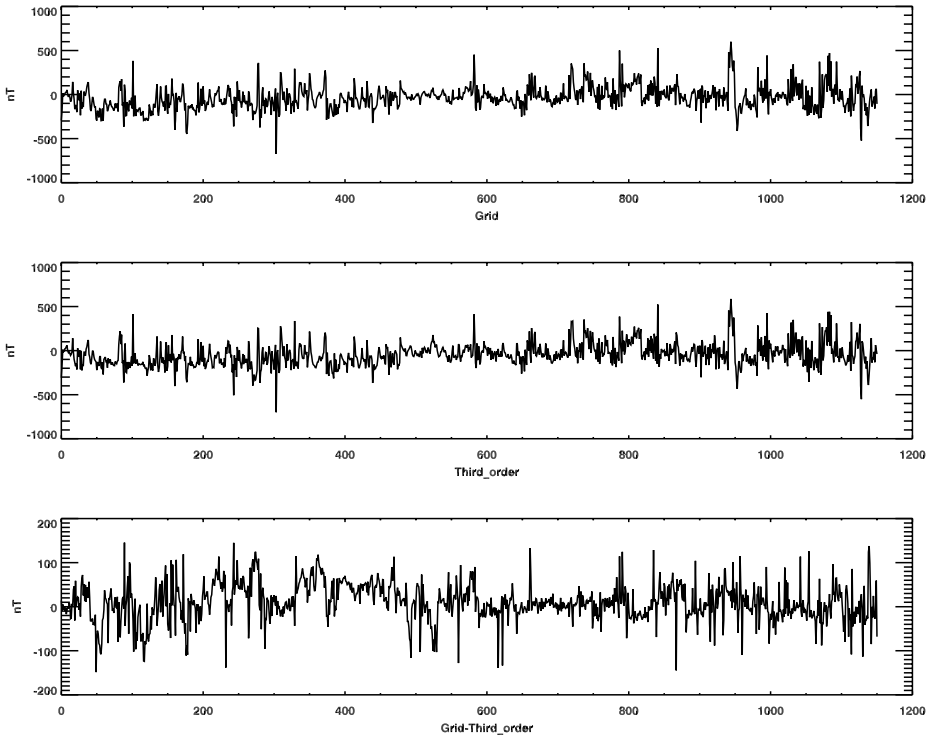

Figure 5.9. Western Australia grid data (top), Third-order data, and their differences (bottom), plotted against the Third-order record number (which equates to time)

The correlation plot is shown in Figure 5.10. There is a very high correlation coefficient, and it is interesting that it lies between the DC shift and tilt and the DC shift, tilt and reference correlation coefficients determined in Chapter 4 for this grid. The line of best fit also confirms the conclusion from the plots in Figure 5.9.

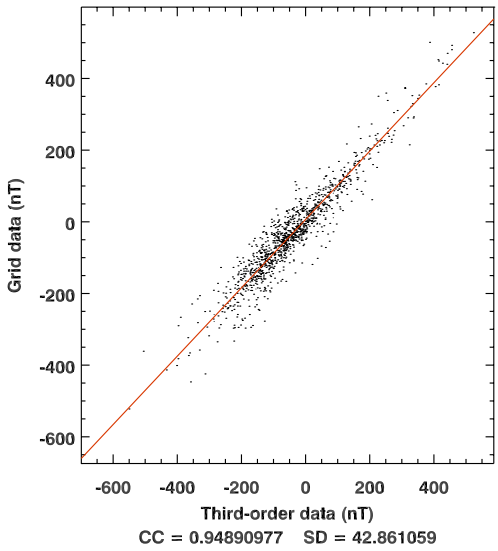

Figure 5.10. The correlation between the Third-order data and the Western Australia final grid data, using diurnally corrected data

There is no significant tilt between the datasets, as the line has a slope close to 1. The standard deviation value of 42.86 also lies between the values obtained from the previous chapter for the last two comparisons. If the AWAGS control traverses are considered as a definitive reference, then the standard deviation here must be a combination of the errors in the merged grid and the errors in the Third-order data. The very long wavelength comparison is confirmed by the plots in Figure 5.11, which shows the degree 1 surfaces of best fit to each of the datasets.

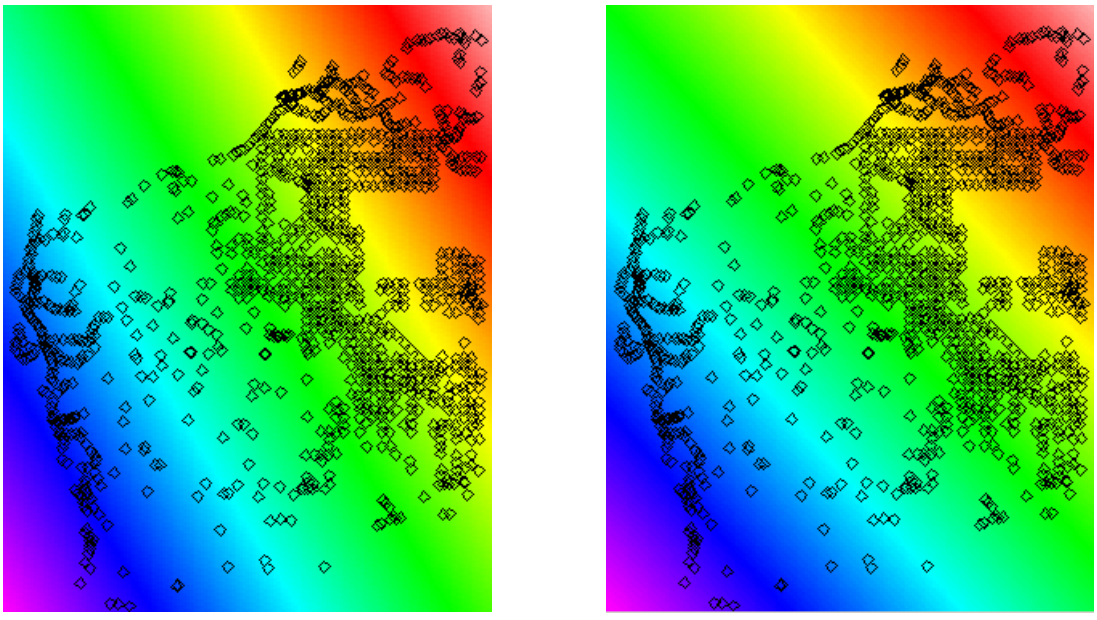

Figure 5.11. The image on the left shows the best fitting degree 1 surface to the Third-order data, and the image on the right the best fitting degree 1 surface to the TMI grid of Western Australia

6. THEORETICAL TESTS OF GRIDMERGE

The methods behind the *Gridmerge* program are new (Minty, 2000; Minty *et al*., in prep.), and it is important to test the program carefully both on synthetic datasets where the result is known, and also on high-quality modern datasets. The latter should merge well together with a minimum of processing, as the data acquisition and reduction technology from raw acquisition to final grids has been consistent for each individual survey. It is also important that high quality grids, when combined with data of a lower quality (usually older survey data), are not contaminated in the merging process by the older quality data.

In Chapter 5 the merging process was tested on a set of high-quality grids from the Yilgarn area of Western Australia. These data merged well, with the exception of the Glengarry/Peak Hill grid, which was erroneously tilted by a degree 1 surface with respect to the test data of the AWAGS flight lines, one traverse of which passes over the grids. Several options within the program were tried, but none of them was successful in removing this tilt. The tilt in the data is of the order of 200 nT, which is unacceptable in terms of providing a reliable long wavelength component to large scale merges of magnetic grid data.

A smaller set of the grids of the Yilgarn area has been extracted to generate a set of ideal test grids. The data of these grids were altered, but the cell sizes and geographic information were retained so they appear to the *Gridmerge* program to be real grids. These grids have known characteristics, such as data mean, variance and degree of warping. Thus, with a set of test data for which we know the ideal result, the program could be tested to its limit.

The first and most obvious test of the program is the levelling of a set of grids which have zero variance but differing means. This set of grids was generated, and the result from *Gridmerge* was as expected; the grids were DC shifted to a common mean so that there was zero difference in their common overlaps.

The second test was to introduce a degree 1 polynomial warp (i.e. a tilted plane) into the centre grid of the test set — this is the data for Duketon (AGSO project P613). A north–south tilt was applied to this grid and then *Gridmerge* was run on the set, using first a DC shift, and then a polynomial correction of degree 1. The results are as follows.

A DC shift correction to the set actually changed the zero difference between the levels of the grids which were originally perfectly level to each other. This is because the mean of the grid which contains the tilt was not zero, and during the singular value decomposition (SVD) DC minimisation process the DC offset of this grid became spread across all the grids, giving them slight DC offsets when they had none to start with. Hence, a DC offset in one grid which is tilted can affect all the grids (see Figure 6.1).

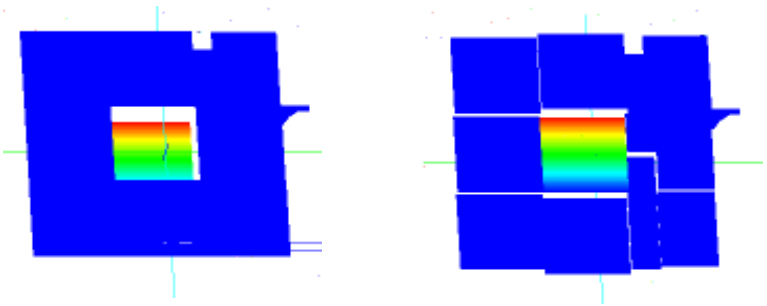

Figure 6.1. These figures provide a perspective view of the DC minimisation process. The figure on the left shows the test data configuration, whereby all the grids in blue have zero means and variances. The central grid has a north–south linear gradient. The figure on the right displays the results after DC minimisation, with the DC offset from the central grid now spread among all the grids.

The real test for this situation is to apply a polynomial correction with *Gridmerge*, allowing for DC shifts as well. Ideally, a degree 1 correction should take out the north–south gradient of the central grid and adjust all the DC levels so there are no overlap differences between any of the grids. Figure 6.2 demonstrates the output of this test. The *Gridmerge* report shows that the final overlap differences are close to zero, the desirable result. However, Figure 6.2 shows that the gradient in the central grid has been spread throughout all the grids, and not just in a north–south direction. Also, although the overlaps are close to zero, the actual means of the grids differ from zero, as is shown by the offsets in the figure. The same scaling factors are applied to every grid, and the reason for the match at the boundaries becomes obvious, as Figure 6.2 shows.

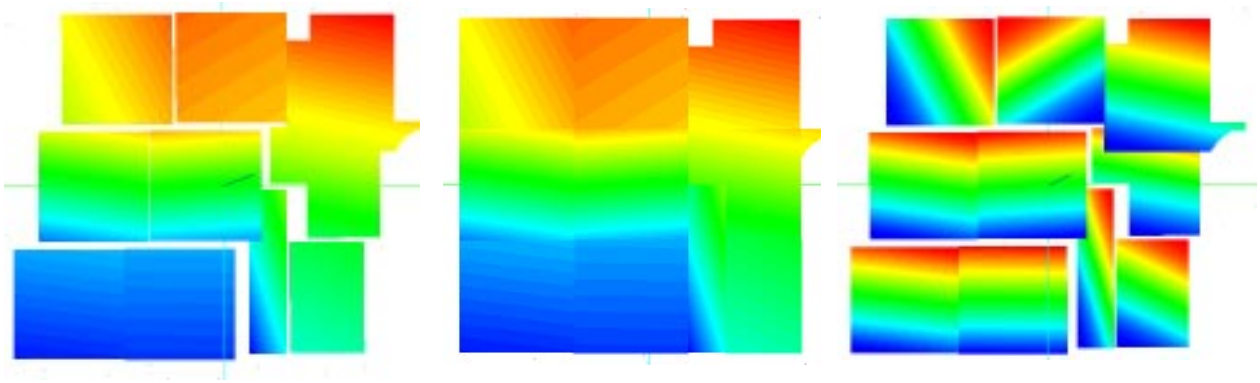

Figure 6.2. Result of polynomial degree 1 adjustment. The figure on the left is a perspective view, and in the centre a view from directly above. These two views have had a linear stretch applied to the whole data range. The figure on the right emphasises the gradients, with each grid individually histogram equalised.

It is interesting to contemplate why the gradients are not all in a north–south direction, the original starting direction. The polynomial applied to the central grid of the test data was computed along columns of the data, so there is absolutely no polynomial component in an east–west direction. A separate test of two grids, one with no polynomial adjacent to one with a polynomial, showed that the slope was taken out perfectly within machine accuracy. The difference plots showing fitted polynomials, which the *Gridmerge* program can display while running, provide a clue to the process. The boundary differences of the overlapping grids are composed not just of two overlapping grids, but also the small end portions from other adjacent grids. The plot of differences across columns shows the perfect horizontal straight line for the two major grid overlaps, but the end grids, which have DC offsets, also show as differences which are significantly different from the main set. Thus, in the fitting of a linear polynomial, the small overlaps at the ends bias the slope significantly away from zero, and hence in the overall iterative process of the program the central slope is spread over all the grids with changes in direction.

The final test involves two grids with gradients, adjacent to each other in the array, one in a north–south direction, and the other east–west. Figure 6.3 displays the results, which are similar to the case above. Neither grid has had the polynomial removed satisfactorily, and the gradients have been spread throughout the entire system. Again the overlap differences are small in most cases, as the central figure illustrates, although not as small as in the case above.

In summary, the user of *Gridmerge* should bear in mind at all times the limitations of the method, be aware of the likely quality of the grids which are being merged, and define appropriate base grids (grids which do not get adjusted) during the process. This will allow the program to adjust grids of lower quality and dubious vintage so they match grids of higher quality. The tests described here are by no means exhaustive, but give some idea of aspects to be aware of.

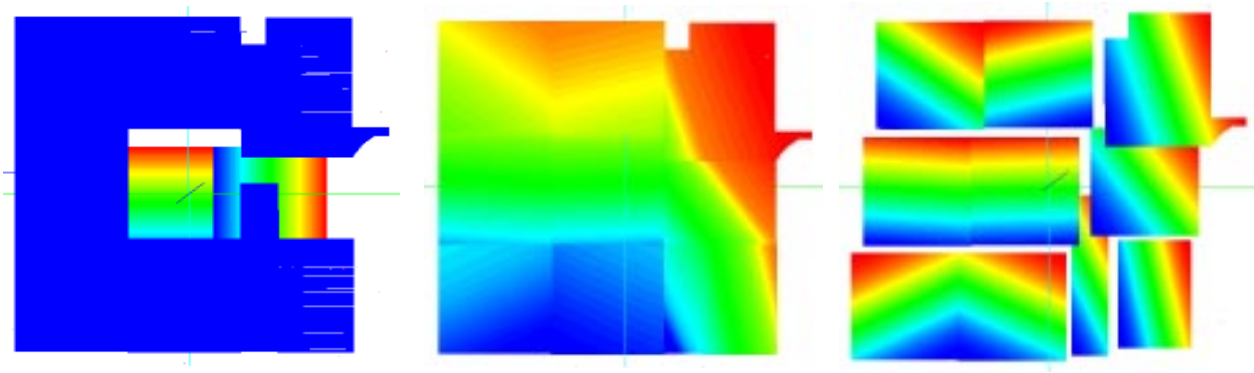

Figure 6.3. The left-hand figure shows the starting position, two grids having gradients. The central figure displays the results by histogram equalisation of the whole data; the right-hand figure has histogram equalisation applied individually to the grids.

7. CONCLUSIONS AND RECOMMENDATIONS

Two datasets, the AWAGS control traverses and the Third-order data, have been described, including their diurnal correction. They can both be used as references and controls for the merging of aeromagnetic grids across Australia.

The AWAGS control traverses are the more precise of the two, and were acquired specifically for this purpose (during January to March, 1990), with diurnal control available from the AWAGS magnetometer deployment. They consist of two large loops around Australia, so there are large areas in between where they do not provide control.

An attempt has been made to diurnally correct the second dataset, the Third-order data, which was collected many years earlier (1967–1974) with much less precision than the AWAGS traverses, over a much longer span of time. The advantage of this dataset is that it covers the whole Australian continent in a semi-random fashion. More exploration of this dataset is required, but on present indications there is very little difference statistically between the diurnally corrected and uncorrected total magnetic intensity data.

The Third-order data have been compared with the AWAGS control traverses, and in a statistical sense the comparison is good. However, the Third-order data cannot be used to provide reliable information for wavelengths less than a few thousand kilometres. In some cases, with judicious selection, the Third-order data can help identify those individual survey grids that are severely tilted.

Several composite Australian aeromagnetic anomaly grids, each resulting from sets of smaller project grids merged using the new *Gridmerge* program, have been compared with both the AWAGS control traverses and the Third-order data. The use of such reference datasets as controls of the actual merging process has also been investigated.

The most favourable comparison is provided by using the AWAGS traverses as a control; so in the case of the Western Australian merged grid the average deviation from the traverses is ±37.5 nT. Without the traverse control, this becomes ±66.15 nT. Figure 3.8 in Chapter 3 shows that the amplitudes of the long wavelengths of the crustal magnetic field at ground level are of the order of 200 nT (this is also confirmed by Wellman *et al.*, 1985). Thus, the standard deviation of the best merging case is 37% of the amplitude of these wavelengths.

Data used to form the composite grids of Western Australia have come from many sources, of widely varying quality and resolution, over a long span of time. Improvement of the comparisons would require a detailed examination of all the grids with respect to the AWAGS traverses and perhaps also the Third-order data, to determine in the first instance whether any are significantly tilted (e.g. the Peak Hill / Glengarry grid which has already been described). If any such cases are found, they should be corrected separately, because the degree 1 process of *Gridmerge* may not accurately remove significant tilts from the desired grids. Judicious selection of base grids (grids which act as references, and are not adjusted), once the quality of all the grids has been determined, will help control tilting in the final merging process. For the continental-scale merge of Western Australia using the AWAGS traverses as a control, there is no overall degree 1 tilt of the dataset.

The examples show that *Gridmerge* provides a very high quality result when modern aeromagnetic data are combined, as is demonstrated by comparisons with both the AWAGS control traverses and the Third-order data. Additional AWAGS-type profiles should be acquired to control any future merging of grids over the large areas of Australia where high quality reference data are not available.

8. REFERENCES

Barritt, S.D., 1993. The African magnetic mapping project. *ITC Journal*, **2**, 122-131.

Barton, C.E., Lilley, F.E.M., Prohasky, W. & McEwin, A.J., 1985. Geomagnetic Workshop, Canberra, 14-15th May, 1985. Programme and Abstracts. *BMR Record* **1985/13**.

Black, P.A., Green, C.M. & Reford, S.W., 1995. A pragmatic approach to continental magnetic compilations. *Annual Meeting Expanded Abstracts*, Society of Exploration Geophysicists, 773-774.

BMR, 1976 – Magnetic map of Australia. Residuals of total intensity 1:2 500 000 scale: *Bureau of Mineral Resources,* Australia.

Campbell, W.H., 1997. Introduction to geomagnetic fields. *Cambridge University Press*.

Chamalaun,F.H. and Barton, C.E., 1990. Comprehensive mapping of Australia's geomagnetic variations: *EOS Trans. Am. Geophys. Union*, **71**, 1867 and 1873.

Chamalaun, F.H. and Walker, B., 1982. A microprocessor-based digital fluxgate magnetometer for geomagnetic deep sounding studies. *J. Geomag. Geoelectr*., **34**, 491-507.

Cheesman, S., MacLeod, I. & Hollyer, G., 1998. A new, rapid, automated grid stitching algorithm. *Exploration Geophysics*, **29**, 301-305.

Chopra, P.N., 1989. The BMR MAGSAT and 3rd-Order geomagnetic ORACLE databases. *BMR Record* **1989/44**.

Dooley, J.C. and McGregor, P.M., 1982. Correlative geophysical data in the Australian Region for use in the MAGSAT project. *Bull. Aust. Soc. Explor. Geophys*., **13**, 63-67.

Dooley, J.C., 1985. Ground control of satellite observations of the geomagnetic field. In:Geomagnetic Workshop, Canberra, 14-15th May, 1985. Programme and Abstracts. *BMR Record* **1985/13**, 21-23.

Finlayson, D., 1973. Isomagnetic maps of the Australian Region for epoch 1970.0. *BMR Report* **159**.

Hinze, W.J., Hood, P.J. and the Committee for the magnetic anomaly map of North America, 1988. Magnetic anomaly map of North America. *Geophysics:the leading edge of exploration*, Nov. 1988, p19.

Hitchman, A.P., 1999. Interactions between aeromagnetic data and electromagnetic induction in the earth. PhD thesis, The Australian National University.

Hitchman, A., Lilley, F.E.M., Campbell, W., Chamalaun, F. & Barton, C.E., 1998. The magnetic daily variation in Australia: dependence of the total-field signal on latitude. *Exploration Geophysics*, **29**, 428-432.

Hone, I.G., Milligan,P.R., Mitchell, J.N., & Horsfall, K., 1997. Australian national airborne geophysical databases. *AGSO Journal of Australian Geology & Geophysics*, **17(2)**, 11-21.

Mackey, T.E., Meixner, A.J. & Milligan, P.R., 2000. Magnetic anomaly map of Western Australia (1:2 500 000 scale): *Australian Geological Survey Organisation*, Canberra.

Milligan, P.R., 1995. Short-period geomagnetic variations recorded concurrently with an aeromagnetic survey across the Bendigo area, Victoria. *Exploration Geophysics*, **26**, 527-534.

Milligan, P.R., White, A., Heinson, G. & Brodie, R., 1993. Micropulsation and induction array study near Ballarat, Victoria. *Exploration Geophysics,* **24**, 117-122.

Milligan, P.R. and Barton, C.E., 1997. Transient and induced variations in aeromagnetics. *AGSO Record* **1997/27**.

Milligan, P.R. and Tarlowski, 1999. The magnetic anomaly map of Australia (3rd Edition), scale 1:5 000 000. *Australian Geological Survey Organisation*, Canberra.

Milligan, P.R., 1999. Total magnetic intensity (reduced to the pole) with east-west gradient enhancement colour pixel-image map of the Curnamona Province, scale 1:500 000, *Australian Geological Survey Organisation*, Canberra.

Milligan, P.R., Direen, N.G. & Shaw, R.D., 2000. Geophysical atlas of the Curnamona Province, 1:2 million scale, *Australian Geological Survey Organisation*, Canberra.

Minty, B., 2000. Automatic merging of gridded airborne gamma-ray spectrometric surveys. *Exploration Geophysics*, **31**, 47-51.

Minty, B.R.S., Milligan, P.R., Luyendyk, A.P.J., and Mackey, T., (in prep). Merging airborne magnetic surveys into continental-scale compilations (in preparation).

Parkinson, W.D., 1959. Directions of rapid geomagnetic fluctuations. *Geophys. J. R. astr. Soc*., **2**, 121-138, 1971.

Parkinson, W.D., 1962. The influence of continents and oceans on geomagnetic variations. *Geophys. J. R. astr. Soc*., **6**, 441-449, 1962.

Reford, S.W., Gupta, V.K., Paterson, N.R., Kwan, K.C.H.& MacLeod, I.N., 1990. The Ontario master aeromagnetic grid: a blueprint for detailed magnetic compilation on a regional scale. *Annual Meeting Expanded Abstracts*, Society of Exploration Geophysicists, 617-619.

Richardson, L.M., 2001. Index of airborne geophysical surveys (fifth edition). *AGSO Record* **2001/14**.

Tarlowski, C., Simonis, F. & Milligan, P.R., 1992. The magnetic anomaly map of Australia. *Exploration Geophysics*, **23**, 339-342.

Tarlowski, C., Simonis, F. & Milligan, P.R., 1993. The magnetic anomaly map of Australia, scale 1:5 000 000. *Australian Geological Survey Organisation*, Canberra.

Tarlowski, C., Milligan, P.R. & Mackey, T., 1995. Magnetic anomaly map of Australia (2nd Edition), scale 1:5 000 000. *Australian Geological Survey Organisation,* Canberra.

Tarlowski, C., McEwin, A.J., Reeves, C.V. & Barton, C.E., 1996. De-warping the composite aeromagnetic anomaly map of Australia using control traverses and base stations. *Geophysics*, **61(3)**, 696-705.

Tarlowski, C., Gunn, P.J. & Mackey, T., 1997. Enhancements of the magnetic map of Australia. *AGSO Journal of Australian Geology & Geophysics*, **17(2)**, 11-21, 77-82.

Tucker, D .H., Hone, I.G., Downie, A., Luyendyk, A., Horsfall, K. & Anfiloff, V., 1988. Aeromagnetic regional survey of onshore Australia. *Geophysics*, **53**, 254-265.

van der Linden, 1971. Third-order regional magnetic surveys in eastern Australia, 1968 and 1969. *BMR and Geophysics*.

Wellman, P., Murray, A.S. & McMullan, M.W., 1985. Australian long-wavelength magnetic anomalies. *BMR Journal of Australian Geology & Geophysics*, **9**, 297-302.

Welsh, W. and Barton, C.E., 1996. The Australia-wide array of geomagnetic stations (AWAGS): data corrections. *AGSO Record* **1996/54**.

Whellams, J.M., 1996. Spatial inhomogeneity of geomagnetic fluctuation fields and their influence on high resolution aeromagnetic surveys. PhD thesis, The Flinders University of South Australia.